ISTANBUL TECHNICAL UNIVERSITY ★ GRADUATE SCHOOL

OPTIMIZATION DESIGN PARAMETERS OF DUAL MASS FLYWHEEL COUPLED WITH A NON-LINEAR ELASTIC PATH

M.Sc. THESIS

Gökay KARAKUŞ

Department of Mechanical Engineering

Automotive Programme

JUNE 2023

ISTANBUL TECHNICAL UNIVERSITY ★ GRADUATE SCHOOL

OPTIMIZATION DESIGN PARAMETERS OF DUAL MASS FLYWHEEL COUPLED WITH A NON-LINEAR ELASTIC PATH

M.Sc. THESIS

Gökay KARAKUŞ
(503191705)

Department of Mechanical Engineering

Automotive Programme

Thesis Advisor: Assoc. Prof. Dr. Osman Taha Şen

JUNE 2023

İSTANBUL TEKNİK ÜNİVERSİTESİ ★ LİSANSÜSTÜ EĞİTİM ENSTİTÜSÜ

LİNEER OLMAYAN ELASTİK YOL İLE ÇALIŞAN ÇİFT KÜTLELİ VOLANIN TASARIM PARAMETRELERİ OPTİMİZASYONU

YÜKSEK LİSANS TEZİ

Gökay KARAKUŞ
(503191705)

Makina Mühendisliği Anabilim Dalı

Otomotiv Programı

Tez Danışmanı: Doç. Dr. Osman Taha ŞEN

HAZİRAN 2023

Gökay Karakuş, a M.Sc. student of İTU Graduate School student ID 503191705, successfully defended the thesis entitled "OPTIMIZATION DESIGN PARAMETERS OF DUAL MASS FLYWHEEL COUPLED WITH A NON-LINEAR ELASTIC PATH", which he prepared after fulfilling the requirements specified in the associated legislations, before the jury whose signatures are below.

Thesis Advisor :	**Assoc. Prof. Dr. Osman Taha Şen** İstanbul Technical University	.....
Jury Members :	**Prof. Dr. Özgen Akalın** Istanbul Technical University	.....
	Prof. Dr. Tarkan Sandalcı Yıldız Technical University	.....

Date of Submission : 21.05.2023
Date of Defense : 23.06.2023

To my family,

FOREWORD

I would like to thank my advisor Assoc. Prof. Dr. Osman Taha ŞEN for his big support, understanding and patience, not only during this study but also during graduate education and undergraduate education of Mechanical Engineering, and Automotive Program.

I also would like to thank my wife, N. Dilge Karakuş, for being with me throughout this master's thesis and for never missing her support.

I also would like to acknowledge my friends, my teachers and everyone who encouraged me to succeed in thesis study. Moreover, I am very grateful to my family, who has always supported me and has a great importance in my life.

June 2023

Gökay KARAKUŞ
(Mechanical Engineer)

TABLE OF CONTENTS

Page

ABBREVIATIONS

1D	**:** One Dimensional
3D	**:** Three Dimensional
CAD	**:** Computer Aided Design
DFTM	**:** Discrete Fourier Transform Matrix
DMF	**:** Dual Mass Flywheel
DOF	: Degree of Freedom
FEM	**:** Finite Element Method
ICE	**:** Internal Combustion Engine
I6	: Inline-6
MDOF	: Multi-degree of Freedom
MHBM	**:** Multi-term Harmonic Balance Method
NVH	: Noise, Vibration, and Harshness
ODE45	**:** Ordinary Differential Equations45 (A function in Matlab)
RPM	: Revolutions per minute
SAE	: Society of Automotive Engineers
SMF	**:** Single Mass Flywheel

SYMBOLS

a_1, a_2	: Unknown Fourier coefficient vectors
c_1, c_2	: Damping coefficient
CR	: Damping ratio
I_1, I_2	: Inertia
IR	: Inertia ratio
J	: Jacobian matrix
k_1, k_2	: Stiffness coefficient
k_{nl}	: Non-linear stiffness coefficient
KR	: Stiffness ratio
R_1, R_2	: Residue functions
T_e	: Engine torque
t	: Time
w	: Angular velocity
ζ	: Damping factor (non-dimensional parameter)
θ_1, θ_2	: Angular displacement
$\dot{\theta}_1, \dot{\theta}_2$	: Angular speed
$\ddot{\theta}_1, \ddot{\theta}_2$	: Angular acceleration
α	: Non-linear path ratio
Ψ	: Linear independent variable transformation term
Γ	: Discrete Fourier transform matrix

LIST OF TABLES

Page

LIST OF FIGURES

Page

OPTIMIZATION DESIGN PARAMETERS OF DUAL MASS FLYWHEEL COUPLED WITH A NON-LINEAR ELASTIC PATH

SUMMARY

Today, expectations from automotive industry are high in the fields of performance, comfort, economy and environmental protection. That is why, the automotive industry must have a knowledge, experience, development processes, and strong research. Hence, the design of the components that transmit power from the internal combustion engine to the wheels via axes in a vehicle are crucial research topics. The flywheel, which is the primary element in power transmission system, works in engine in order to reduce the speed fluctuations on the crankshaft. Along with the studies in the field of flywheel development, dual-mass flywheels have been started to be used as an alternative to the single-mass flywheel. Briefly, the dual mass flywheel can be defined as the combination of two single mass flywheels. The spring damper system is combined with these two single mass flywheels. The dual-mass flywheel, which is used in diesel engines, is thought to have favorable effects on the dynamics of the power transmission system compared to the single-mass flywheel.

In 1985, the first dual mass flywheel (DMF) was manufactured in automotive sector. In begin, dampers in flywheel were not lubricated and the springs are stand away from outside and created some wear problems. In 1987, DMF is lubricated with grease oil for the first time. Service life problem was no longer an issue thanks to grease oil application.

Around 1989, arc spring damper was innovation for the DMF, and it had pretty much solved all resonance problems. Alson manufacturing costs were continually reduced. The primary mass of flywheel was made by casting or forged steel at first production batches. Over time, the primary mass was formed from sheet metal parts by metal-forming specialists. In 1995, folded masses were developed from sheet metal in order to increase inertia moment of primary mass of flywheel. This development led to the widespread use of the DMF.

However, there is some disadvantages such as cost, the achievable improvements are seen clearly, therefore, DMF are used widespread in vehicles. There are some advantages of dual mass flywheel such as isolation from torsional vibration, relief of transmission and crankshaft.

Within the scope of this study, firstly, give information about flywheel, parts of dual mass flywheel and its advantages. Then, while engine is running, the working principles of dual mass flywheel is mentioned. Also, the single mass flywheel and dual mass flywheel are compared and it has been observed that the resonance regions are reduced below the engine idle speed with the use of dual-mass flywheel. After all crucial information was explained, mathematical model of DMF is built. The model was solved in Matlab for all optimization. Sensitivity analysis was done in order to

determine the parameter effects on system. The design parameters were determined as stiffness ratio, damping ratio and inertia ratio. Also, the system was running on non-linear cubic path, that is why, non-linear stiffness ratio is also important parameter to examine system correctly. The primary body represent not only primary flywheel itself but also engine side dynamic properties. The system has 2 degrees of freedom and torque input was only from engine-side, in contrast, transmission side was assumed constant. Thus, any obtained displacement datas from secondary mass means the value of penetrate of vibration to transmission side.

In this paper, the heavy-duty engine, which is used for truck or marine application, was examined and torque values were obtained from I6 truck engine test datas. According to obtaining test datas, output of two mass were examined thanks to torque input and another defined parameter such as inertias, damping coefficients and stiffening coefficients. Also, dual mass flywheel was investigated and chose feasible flywheel from Geislinger supplier booklet. When selecting the appropriate flywheel, dimensionally SAE standards were taken into account. SAE-1 flywheel is chosen since selected engine has SAE-1 design.

In the second part of the thesis, the mathematical calculations made behind the model and the mathematical infrastructure are explained. First of all, create equation of motions according to mathematical model. Then, equations of motion are created, moreover, equations were converted to non-dimensional because of non-linear term in equations. For solving system in frequency domain, the multi-term harmonic balance method (MHBM) is used to built steady-state response in system coupled with non-linear cubic path. Hence, non-dimensional equations convert to nonlinear governing equations with using MHBM.

In third section in this paper, the important system parameters were changed, and system response was analyzed according to parameter deviations. Stiffness, damping and inertia values were modified on system, and system response was argued at third section in detail. This system analysis was done both in time and frequency domains.

The final chapter gives a last comment about results obtained from nonlinear model in time and frequency domains.

LINEER OLMAYAN ELASTİK YOL İLE ÇALIŞAN ÇİFT KÜTLELİ VOLANIN TASARIM PARAMETRELERİ OPTİMİZASYONU

ÖZET

Günümüzde, otomotiv endüstrisinde çevre koruma, konfor, sürüş dinamikleri, performans ve ekonomi anlamında beklentiler çok yukarıdadır. Bu yüzden otomotiv sektöründe bilgi birikimi, tecrübe, Ar-ge çalışmaları bu beklentiyi destekler nitelikte olmalıdır. İçten yanmalı motordan elde edilen gücün akslara oradan da tekere iletilmesi konusunda birçok önemli çalışma bulunmaktadır. Güç aktarım sisteminde en önemli parçalardan biri olan volanın görevi motor tarafında oluşan hız/tork dalgalanma düzeyini düşürmektir. Volan üstünde yapılan çalışmalarla paralel olarak sadece tek kütleli volan değil aynı zamanda çift kütleli volanın da kullanılabileceği ortaya çıkmıştır. Çift kütleli volan kısaca iki adet tek kütleli volanın arasında yaylı amortisör sistemi ile birbirine bağlanmış hali olarak kabul edilebilir. Genelde güç yoğunluğu fazla olan motor tiplerinde kullanıldığından dolayı, dizel motorlarda daha yaygın olduğu görülmektedir ve güç aktarım sistemi dinamikleri üzerinde olumlu etkilere sahip olduğu düşünülmektedir.

Çift kütleli volanın tarihçesine bakarsak, ilk olarak 1985 yılında üretildi. Başlangıçta volan içindeki amortisörler yağlanmadan kullanılmıştır. Ayrıca yaylar dışarıdan bağlantılı olduğu için bazı aşınma problemleri oluşturuyordu. 1987 yılına gelindiğinde, çift kütleli volan ilk kez gres yağı kullanılarak yağlanmıştır. Böylelikle çift kütleli volanın ömür problem ortadan kaldırılmıştır.

1989 yılında çift kütleli volanlarda ark yaylı sönümleyici kullanılmaya başlandı ve bunun sayesinde rezonans problemleri çözüldü. Ayrıca yapılan her bir geliştirme ile üretim maliyetleri de sürekli azalmaktaydı. Volanın ana (birinci) kütlesi ilk üretim yapılırken döküm veya dövme çelikten yapılmıştır. Ancak zaman geçtikçe birincil kütle sac parçalardan oluşturulmaya başlanmıştır. 1995 yılında volanın birincil kütlesinin atalet momentini arttırmak adına sacdan yapılmış katlanmış kütleler (folded masses) geliştirildi. Bu gelişme ile birlikte çift kütleli volanın araçlarda kullanılma sıklığı artmaya başlamıştır.

Çift kütleli volanın çalışma prensibine bakıldığında, bu tez özelinde seçilen volanın 6 adet eğri yayı (arc-spring), 8 adet de yay yatağı bulunmaktadır. Motorun krank eksenine dik eksende bu yay ve yatakları simetrik olarak konumlanmıştır. Dolayısıyla volanın üç yay ve dört yay yatağı var gibi çalışma prensibine değinilecektir.

Sistem sıkışmaya başlamadan önce üç yay birbirine seri olarak bağlıdır. Daha sonra volanın açısal hareketi ile birlikte, üçüncü yay sıkışmaya başlayacak; üçüncü ve dördüncü yatak birbirine yaklaşmaya başlayacak. Bu duruma birinci sıkışma evresi denmektedir. İkinci sıkışma seviyesinde, volanın dönme açısı daha da artmaktadır ve dördüncü yatak, üçüncü yatağa temas edecektir. Bu durumda üçüncü yay daha fazla sıkışamayacaktır ve sistemde sadece birinci ve ikinci yaylar çalışmaya devam

edecektir. Üçüncü sıkışma seviyesi ise sistemin en fazla çalışabileceği aralığı gösterir. Üçüncü sıkışma evresinin sonunda artık son iki yay yatağı ikinci yatak ile temas etmektedir. Bunun sonucunda ikinci yay da sıkışamaz hale gelmektedir. Bu evre, seçilen volanın maksimum çalışma aralığını gösterir.

Tek kütleli volan ile karşılaştırıldığında, çift kütleli volanın maliyet gibi dezavantajları olsa da elde edilecek potansiyel iyileştirmeler dikkate alındığında çift kütleli volanın kullanımı yaygınlaşmıştır. Bu avantajlardan tezde detaylıca bahsedilecek olup kısaca, burulma titreşimini düşürme, izolasyon, şanzımana gelen yüklerin azaltılması, krank miline gelen yüklerin azaltılması denebilir.

Bu tez çalışmasında öncelikle volan hakkında bilgi verilmiştir. Daha sonra çift kütleli volanın parçalarından ve avantajlarından bahsedilmiştir. Devamında motor çalışırken, çift kütleli volanın çalışma prensiplerinden ve davranışından bahsedilmiştir. Ayrıca tek kütleli volan ile karşılaştırılmış olup, çift kütleli volan kullanımı ile motorun rezonans bölgelerinin motor rölanti devrinin altına düşürdüğü gözlemlenmiştir. Tüm bu önemli bilgiler açıklandıktan sonra, çift kütleli volanın matematiksel modeli oluşturulmuştur. Modelde yapılan tüm analizler Matlab program ile yapılmıştır. Seçilen parametrelerin sistem üzerindeki etkilerini belirlemek için duyarlılık analizi yapılmıştır. Seçilen tasarım parametrelerinden kısaca bahsedecek olursak rijitlik oranı, sönümleme oranı ve atalet oranıdır. Bu oranlardaki yapılan optimizasyon çalışmasında değişiklikler ikinci kütle üzerinde yapılmış olup, oran artış azalışı bu şekilde sağlanmıştır. Ayrıca sistem lineer olmayan kübik bir yolda çalıştığı için lineer olmayan rijitlik oranı da sistemi doğru incelemek için önemli bir parametredir. Oluşturulan matematik modeline göre birincil kütle, sadece kendisi için değil aynı zamanda motor tarafının dinamik özelliklerini de temsil etmektedir. Bu yüzden sistem 3 yerine 2 serbestlik derecesine sahiptir ve tork girişi motor tarafından verilmiştir. Burada asıl titreşim dengesizliğinin yaratıldığı bölgenin içten yanmalı motor tarafında olması esas alınmıştır. İçten yanmalı motorda her bir silindir içi patlamada oluşan bu hız ve tork salınımı matematik modelde belirtilmeye çalışılmıştır. Motor girişine göre bakıldığında transmisyon tarafındaki açısal yer değiştirmeler stabil kaldığından modelin transmisyon ile bağlantısı sabit kabul edilmiştir. Analiz çıktılarına ilerleyen bölümlerde detaylı bakılacaktır. Ancak kısaca değinilmek istenirse, seçilen sistemde atalet oranlarını (I_2/I_1) azalttığımızda sistemi tanımlayan kütlelerin genliklerinin düştüğünü görebiliriz. Sönüm oranının etkisi ise ters orantılıdır. Yani sönüm oranını arttırdığımız zaman, sistemdeki kütlelerin hareket genlikleri düşüş göstermektedir. Yay kat sayısı oranı diğer parametrelerin aksine (k_1/k_2) olarak alındığı için oranı arttırmak için ikinci yayın kat sayısını düşürmek gerekmektedir. Yay katsayı oranı arttırılırsa sistemin deplasmanı da düşmektedir.

Bu çalışmada incelenen motor, kamyon ve deniz taşıtlarında kullanılan ağır hizmet motorları ile aynı prensiptedir. Bu tezde kullanılan tork değerleri bilgisayar ortamında elde edilmiş I6 kamyon motoru verileridir. Elde edilen test verilerine göre, tork girişi ve ataletler, sönümleme katsayıları ve rijitlik katsayıları gibi tanımlanmış parametreler sayesinde iki kütlenin yer değiştirme cevapları incelenmiştir. Ayrıca çift kütleli volan seçilirken birçok tedarikçi incelenip, Valeo ya da Geislinger kitapçıklarından sisteme uygun bir çift kütleli volan bulunabilmektedir. Uygun volan seçilirken boyutsal olarak SAE standartları dikkate alınmıştır. Seçilen motorun volan-transmisyon tarafında SAE-1 tasarımına sahip olduğu için volan da uygun olarak SAE-1 standardında seçilmiştir.

Tezin ikinci bölümünde ise oluşturulan modelin arka planında yapılan matematik hesapları ve bu hesapların teorisinden bahsedilmiştir. Öncelikle matematiksel modelin hareket denklemleri oluşturulur. Bu noktada sistem 2 serbestlik derecesine sahip olduğu için 2 adet hareket denklemi kurulması doğrudur. Sistemin bir tarafı transmisyon tarafı olup herhangi bir dış kuvvet ya da tork eklenmemiştir. Sistemin diğer tarafında ise içten yanmalı motor bulunmaktadır ve buradaki tork dalgalanmaları elde edilen test verileri kullanılarak matematik modeline eklenmiştir. Sistem, lineer olmayan kübik yolla birleştirilen hareket denklemlerine sahip olduğu için denklemlerin daha kolay çözülmesi adına boyutsuz hale dönüştürülmüştür. Zaman alanındaki çözümler bu şekilde yapılmış ve tüm parametrelerin etkileri anlatılmak istenmiştir. Bu noktada seçilen parametreler kütlelerin atalet, sönüm ve yay katsayıları oranlarıdır. Ayrıca sistem lineer olmayan bir sistem olduğu için, sistemde ekli olan lineer olmayan yay katsayısı da incelenmiştir. Frekans alanındaki çözümü elde etmek için çok terimli harmonik denge yöntemi (MHBM) kullanılmıştır. Dolayısıyla zaman alanındaki çözümde kullanılan boyutsuz denklemler MHBM kullanılarak dönüştürülmüştür. Buradaki amaç lineer olmayan sistemin sabit durum cevabı (steady-state response) vermesidir.

Tezin üçüncü bölümünde ise önemli sistem parametreleri değiştirilmiş ve parametre sapmalarına göre sistem yanıtı analiz edilmiştir. Rijitlik, sönümleme ve atalet değerleri sistem üzerinde modifiye edilmiş ve sistem tepkisi üçüncü bölümde ayrıntılı olarak tartışılmıştır. Bu sistem analizi hem zaman hem de frekans alanında yapılmıştır.

Son bölümde ise zaman ve frekans alanlarında doğrusal olmayan modelden elde edilen sonuçlar incelenmiştir. Parametrelerin değişikliği sistemi nasıl ve ne kadar etkilediği incelenmiş ve genel olarak son bir yorum belirtilmiştir.

1. INTRODUCTION

Nowadays, the developments in internal combustion engines (ICE) concentrate on getting better the engine performance, less fuel consumption of engine and also reducing emissions. Increasing peak cylinder pressures and modify engine configurations to reach high engine working points. To achieve this, engines can be used less cylinders and worked high power density conditions. Also, with using less cylinder and downsizing engine reduce manufacturing cost. Because of environmental, economical and technical requirements, ICE should modify to using less cylinder, therefore, engines should work with high cylinder pressures. However, this improvement makes a problem in the field of durability of engine components which works under high loads.

These engines have high torque, high power density and high engine speed characteristics, hence, the torsional behavior of system is getting crucial for these engines. Torsional vibrations may create noise, vibration and harshness (NVH), and also some durability problems of system. That is why, torsional vibrations should be reduced to safe zone for engine durability performance.

Heavy duty engines, which operate in marine and truck, have high level torsional vibrations because of high cylinder pressures. In fact, the applications of reducing torsional vibration are major issue for high power density engines. Torsional vibrations, which are generally seen in internal combustion engines, can be prevented with a torsional vibration damper, or they can be resolved by dual-mass flywheel used at the rear end of the crankshaft.

1.1 Motivation

Torsional vibrations of the engine reduce with using dual mass flywheel, when high power density internal combustion engines. In the literature, there are a lot of paper about comparison of single mass to dual mass flywheel. But dual mass flywheel which works on non-linear cubic path is not common study in the literature. The aim of this

paper is that optimize the performance of dual mass flywheel at non-linear cubic working path. After explaining the basic design of flywheel, it would like to build non-linear mathematical model of flywheel and solved equations of motion. Because of all these, the objective of extensive thesis study is solving motion of dual mass flywheel in non-linear cubic path which does not have an overall knowledge in the literature. With this motivation, the effects of whole design parameter are desired to be examined with numerical method.

1.2 Purposes of Thesis

In this paper, dual mass flywheel will be investigated as 2-DOF system. Effects of changing on damping, inertia and stiffness ratios on dual mass flywheel will be determined. The goal of the thesis is that explain the working principle of dual mass flywheel and analyze with different cases in time and frequency domains.

When DFM is built model, some limitations were encountered. The most important restrictions or simplifications are listed below;

- The analysis will be in 1-D model
- Potential energy (gravitational effect) is assumed to less value term with respect to kinetic energy term. So, gravitational energy is neglected.
- Only torsional vibrations are considered.
- In this paper, DMF is just examined with numerical methods. There is no data is gathered from experimental or test benches.
- The input torque is assumed as sine wave.

2. GENERAL REMARKS

2.1 Historical Development of Dual Mass Flywheel

In 1985, the first dual mass flywheel (DMF) was manufactured in automotive sector. The development of DMF is presented in Figure 2.1. In begin, dampers in flywheel were not lubricated and the springs are stand away from outside and created some wear problems. In 1987, DMF is lubricated with grease oil for the first time. Service life problem was no longer an issue thanks to grease oil application.

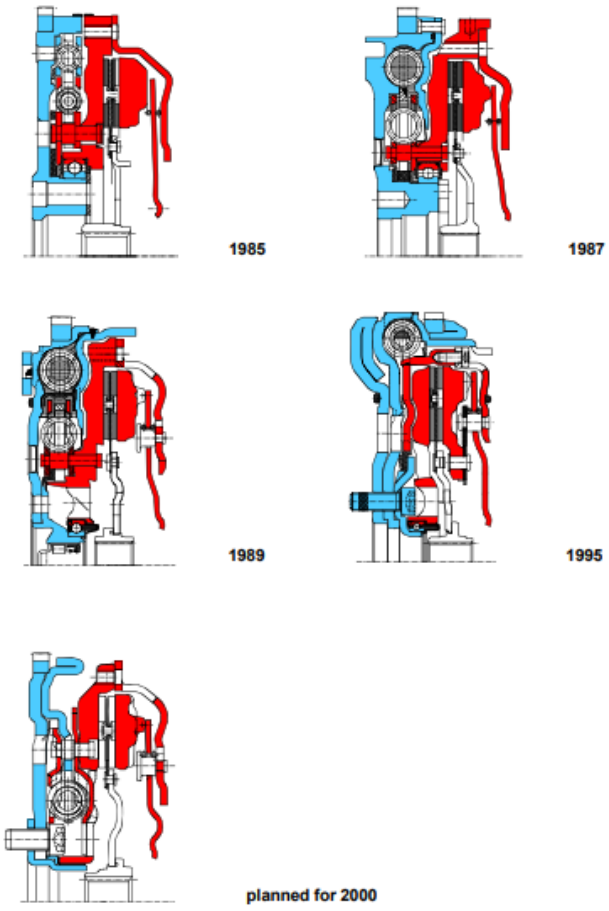

Figure 2.1: Development history of DMF

Around 1989, arc spring damper was innovation for the DMF, and it had pretty much solved all resonance problems. Alson manufacturing costs were continually reduced. The primary mass of flywheel was made by casting or forged steel at first production batches. Over time, the primary mass was formed from sheet metal parts by metal-forming specialists. In 1995, folded masses were developed from sheet metal in order to increase inertia moment of primary mass of flywheel. This development led to the widespread use of the DMF. In Figure 2.2, DMF production increase for German car manufacturers can be seen clearly [4].

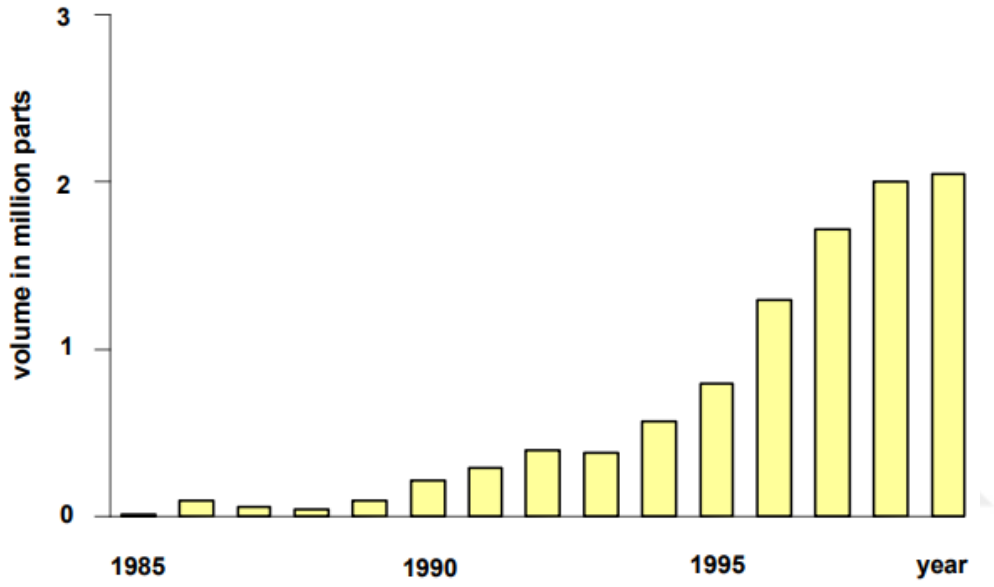

Figure 2.2: Development of DMF production for German car manufacturers.

2.2 Advantages of Dual Mass Flywheel

However, there is some disadvantages such as cost, the achievable improvements are seen clearly, therefore, DMF are used widespread in vehicles. Advantages of dual mass flywheel is described below.

2.2.1 Isolation from torsional vibrations

The main advantage of DMF is the nearly completely isolation of torsional vibrations. In Figure 2.3, there is an angle acceleration comparison of conventional system with a torsion damper and DMF in clutch disc. At low speeds, there is no vibration isolation in clutch disc for with torsion damper.

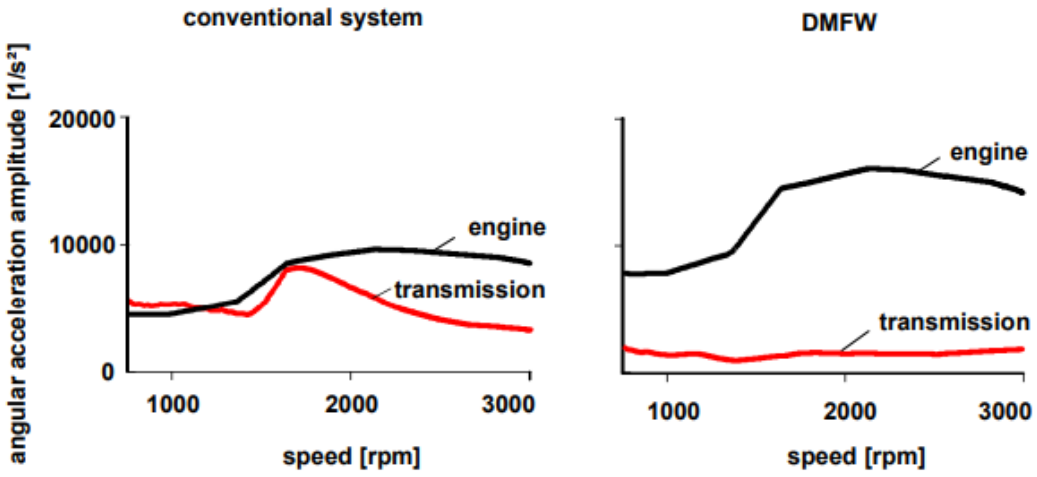

Figure 2.3: Comparison of torsional vibration isolation in conventional system to DMF.

On the contrary, DMF is almost isolate all torsional vibrations and engine irregularities. No longer resonance is not occurred in driving range. The transmission input shaft and also the secondary flywheel side operate almost uniform, that's why, gear rattle is not occurred longer.

In DMF system, the primary mass of flywheel has lower than the conventional one, therefore, the irregularity of engine itself is getting bigger with DMF. Hence, the engine accessories drive should be retuned occasionally.

During especially low-speed driving, DMF leads to low fuel consumption thanks to good vibration isolation. Many modern vehicles, engines have generally flat torque curve, therefore, many manufacturers prefer DMF.

2.2.2 Transmission relief

Another advantages of DMF is effect on transmission stress relief. The stresses on transmission and drive train are relieved thanks to lack of engine irregularities.

In Figure 2.4, the full load torque curve of typical diesel engine is represented with black curve. With additional dynamic torques, black curve is superimposed to red curve and clearly seen the dynamic torques can generate more than 10% extra load on engine.

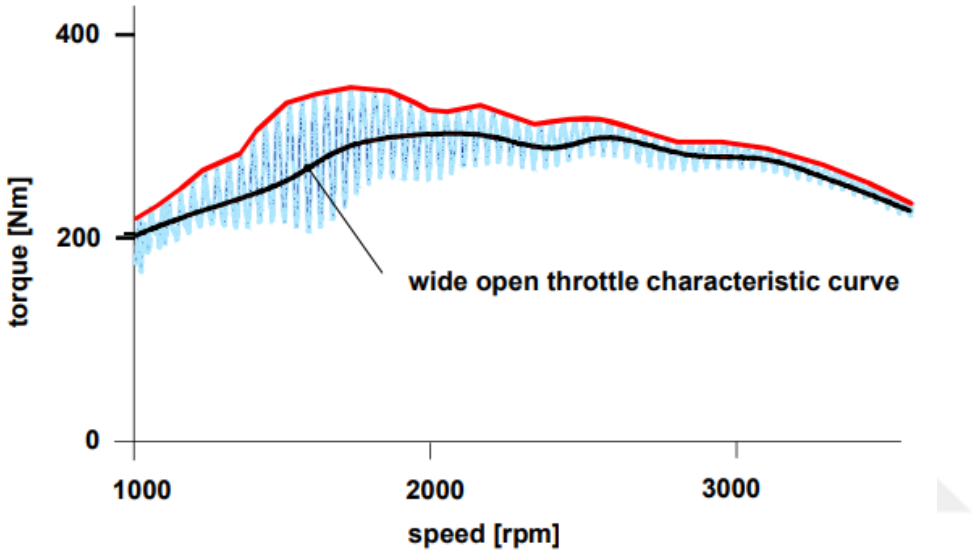

Figure 2.4: Increase of full throat torque curve due to engine irregularities.

2.2.3 Crankshaft relief

DMF completely change the vibration characteristic of the crankshaft. For conventional system without secondary mass, flywheel is rigidly connected with crankshaft and flywheel has also clutch. The large inertia of whole flywheel assembly generates high reaction forces on the crankshaft.

In DMF system, secondary mass is not rigidly connected to flywheel. It is loosely connected via roller bearing to first flywheel mass. Therefore, flywheel has no much bigger bending load than conventional one.

The primary flywheel of DMF has much less mass according to conventional flywheel and is also elastic, like a flexplate. Resonance caused by bending and torsional form

change with DMF and crankshaft is generally relieved. It is clearly seen in Figure 2.5 that the bending and torsional vibrations are less with DMF.

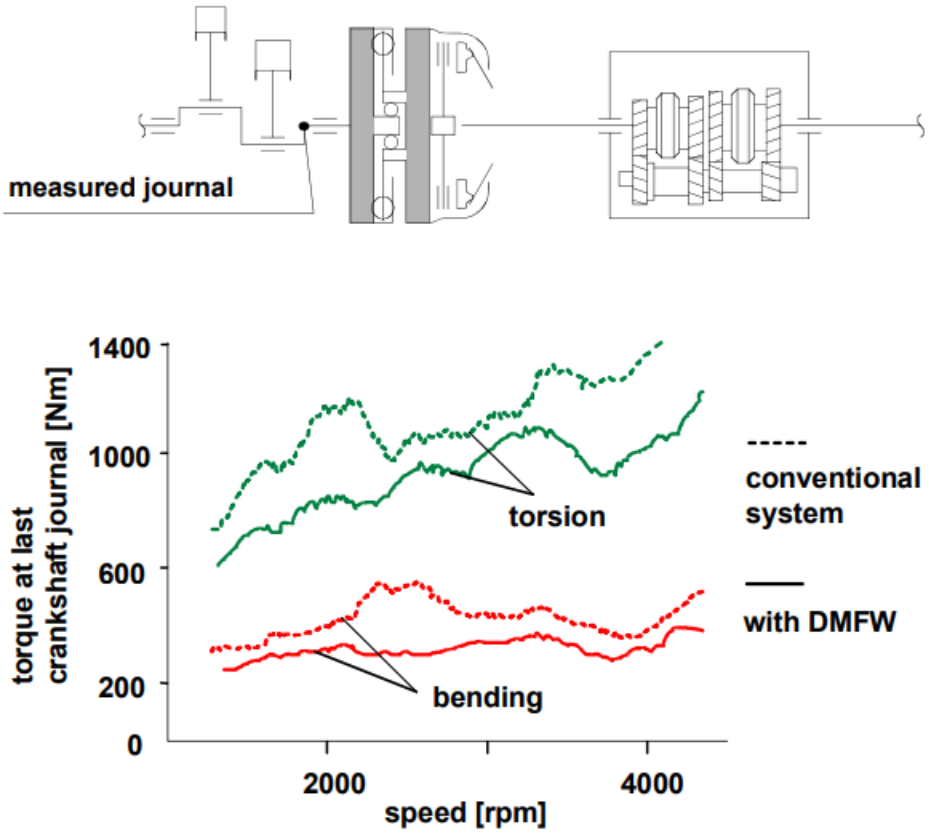

Figure 2.5: Comparison of torsion and bending vibration of conventional system to DMF.

2.2.4 Engine start

DMF is good choice for vibration isolation thanks to shift the resonance frequency to below idle speed successfully via secondary flywheel mass.

In another aspect, engine speed should pass the resonance frequency range for each start of engine. Because of this problem, during the development of DMF, resonance amplitudes should be considered in design.

The bigger inertia creates the higher torque, therefore, only three or four-cylinders diesel engines is more available for DMF application. Engine frictions, load friction and arc spring friction create damping effect. Because, these damping effects can diminish the isolation, there are some limits in engine type and number of cylinders.

To eliminate starting resonance range, electronically controlled engines is developed. According to researches, the starting torque of engine is important factor to resonance form. The more starter speed is achieved with the more engine acceleration. It means that engine pass through the range of below idle speed faster. In Figure 2.6, poor starting behavior is represented.

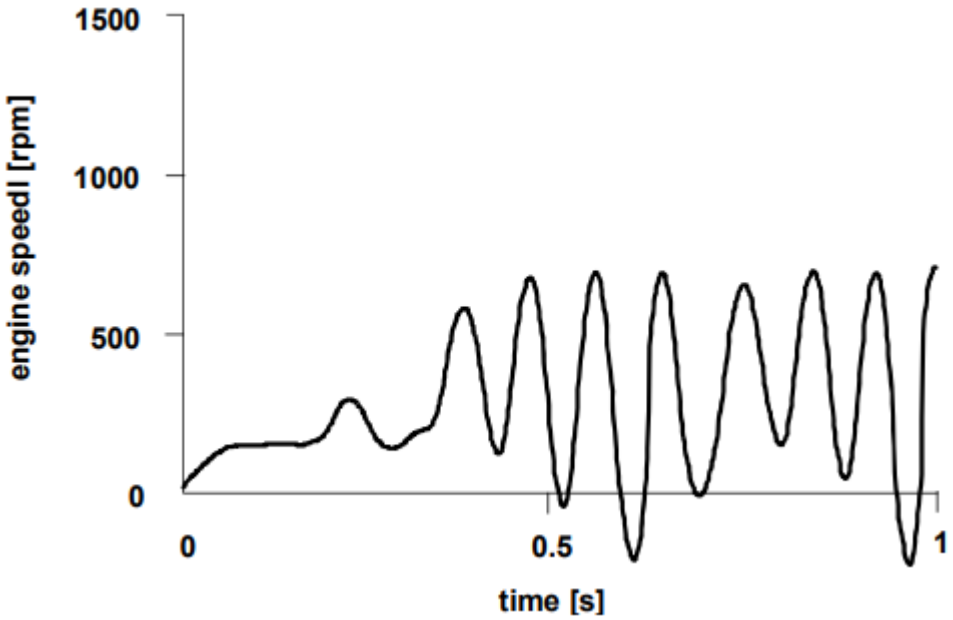

Figure 2.6: Poor starting behavior literature review.

2.2.5 Dual mass flywheel

In vehicles, power package which includes transmission, engine and powertrain is a complex multi-degree of freedom (MDOF) non-linear system, which is seen schematically in Figure 2.7. The transmission section (driveline) is exposed enormous vibration and noise problems because of the torque variation of engine. Furthermore, transient shock and high frequency vibration are happened due to torsional vibration. Torsional vibration in the transmission system will cause the components in this system to be subjected to large torsional loads. The performance and service life of transmission components will be reduced due to knocking on transmission cavities such as splines and gears. Hence, it is very important to be precise during the modeling of the vehicle transmission system and to examine the performance simulation and damping methods.

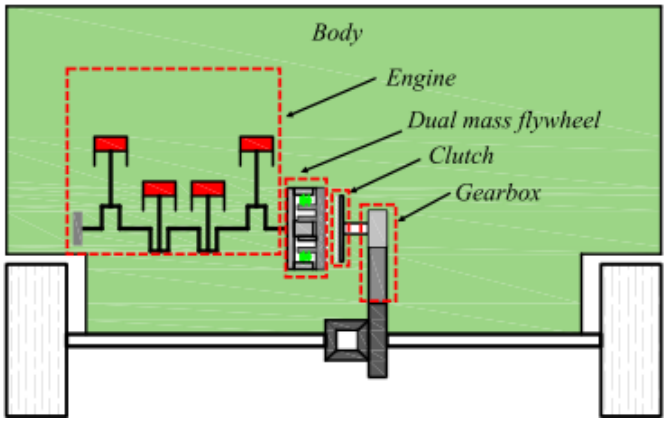

Figure 2.7: Scheme of power transmission system.

The dual-mass flywheel is composed of the first mass connected to the crankshaft and the second mass connected to the transmission input shaft. These two masses are assumed independent flywheels and these independent flywheels were interconnected by spring-damper system. Masses on flywheel are supported by the bearing or sliding bearing to be turned properly to the other side. The ring gear is triggered by the starter gear on the first mass in the flywheel. The first mass cover creates the necessary space for the first mass of the flywheel to perform its circular motion inside the spring channel. The helical springs have a curved shape to fit into the guides in the spring channels. The drive flange which is transmitted engine torque has been riveted to the second mass. The ears of flange match between the spring grooves of the first mass. The exploded picture of dual mass flywheel can be shown in Figure 2.8.

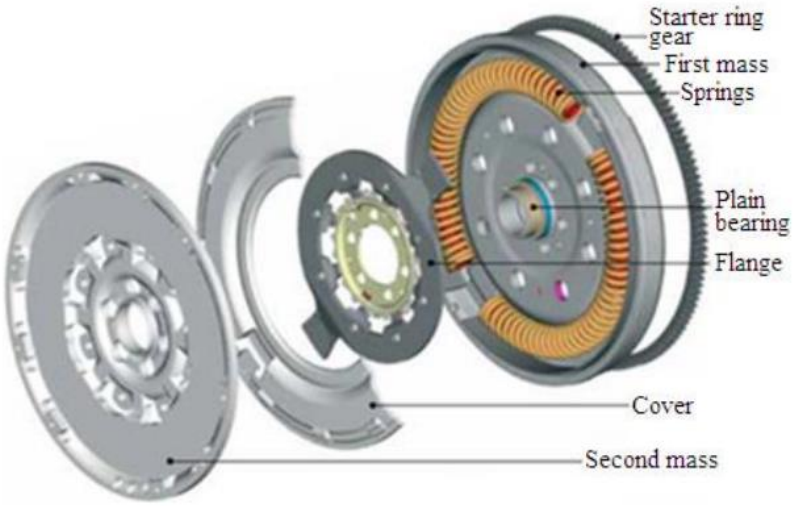

Figure 2.8: Disassembled of dual mass flywheel.

Torsional damping springs, which are located on the clutch disc of mechanical clutch system, protect powertrain components from torsional vibrations caused by speed irregularities in the engine. These springs are not capable of damping the torsional vibrations transferring to gearbox. At low engine speeds, this phenomenon leads to resonance vibration. This resonance causes additional loads on gearbox and also makes extra noise problem. Engine and powertrain work together under the flicker-free operation at lower engine speeds. The dual-mass flywheel has its own spring-damper system and thanks to this, resonance rpm is shifted to below idle engine speed.

Dual-mass flywheel consists of primary flywheel, shock absorber, drive plate, secondary flywheel, compensation device, inertia balance mechanism, bearing inner ring, pressure plate and end cover as it is shown in Figure 2.9. The shock absorber, which includes springs and spring seats, is located in the internal space of primary flywheel and the drive plate is bolted to the secondary flywheel. The compensation device and the inertia balance mechanism are mounted on the secondary flywheel, and the bearing inner ring and three bearing blocks are put in the internal space of the secondary flywheel and closed by the pressure plate. Furthermore, bearing inner ring and end cover are connected with bolts and this connection forms a journal bearing, which is fixed with the primary flywheel.

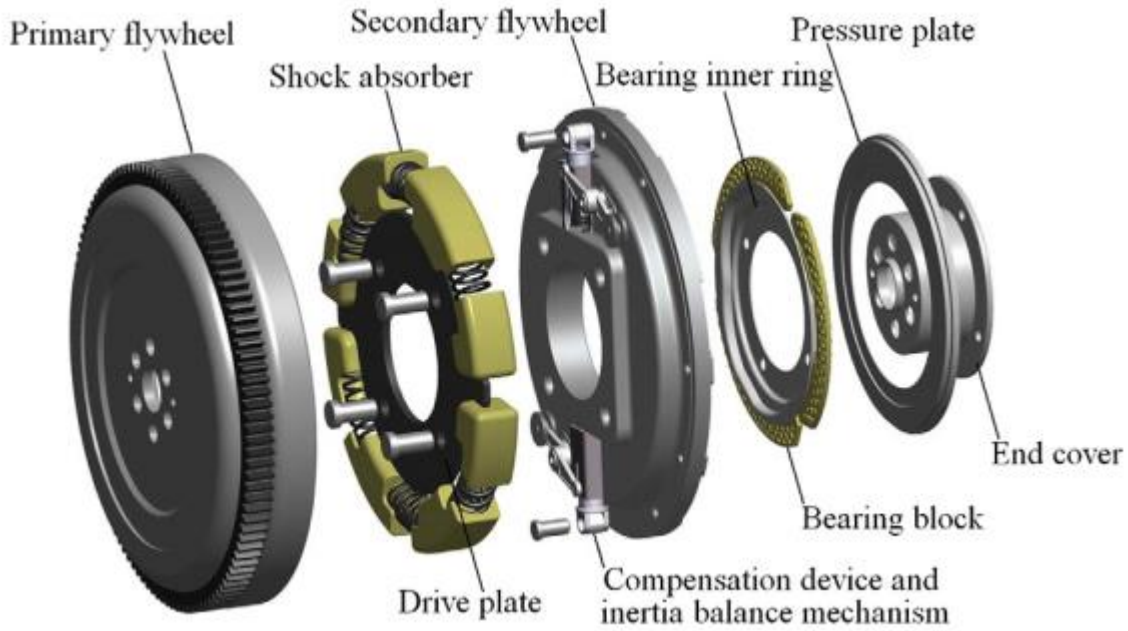

Figure 2.9: Detailed of dual mass flywheel.

Figure 2.10 shows the change in stiffness of DMF. Figure 2.10a is the initial state. During working DMF, it is assumed that the secondary flywheel rotates relative to the primary flywheel. The spring seat 1 rotates due to the movement of the drive plate which is fixed on the secondary flywheel. While there is no contact between all the spring seats as it is shown in Figure 2.10b, then the springs 1, 2 and 3 inserted between these spring seats are connected in series, hence creating the first stage stiffness of the DMF. On the other hand, after rotating with specific angle, the spring seat 3 comes into contact with the spring seat 4. In this case, when the springs 1 and 2 are in series, the spring 3 is no longer compressed during spring series 1&2 is still compressed. Thus, the second stage stiffness is produced as it is shown in Figure 2.10c. Also, when spring seat 2 is connected to spring seat 3 (already in contact with spring seat 4), only the spring 1 with the greatest stiffness can continue to be pressed until spring seat 1 comes into contact with spring seat 2 (i.e., until the torsion angle is reached to its maximum value) and thus the third stage stiffness arises as shown in Figure 2.10d.

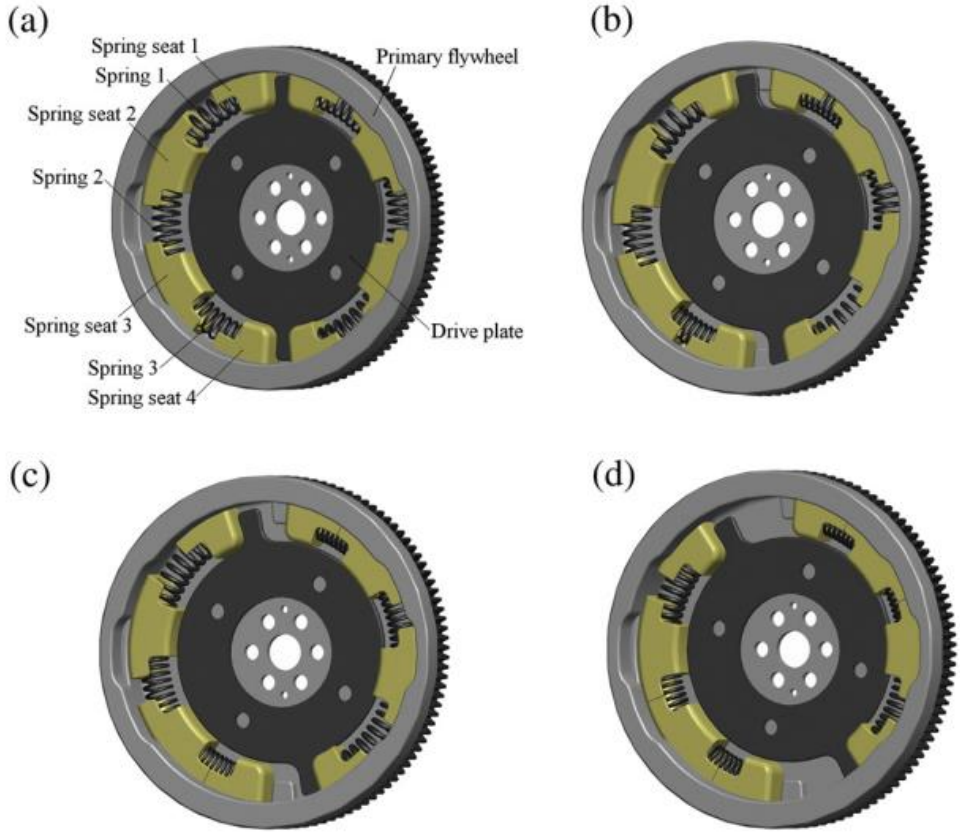

Figure 2.10: The working stages of DMF (a)initial, (b)first stage stiffness (c)second stage stiffness (d)third stage stiffness.

2.2.6 Comparison of single mass flywheel and dual mass flywheel

To understand differences between SMF and DMF, two different models have been figured in this section. These both models include gear box, clutch disc and flywheel. In Figure 2.11 and 2.12, SMF and DMF applications are shown as schematic. Unlike DMF application, the clutch system of the model with SMF has torsional springs. In DMF application, power transmission has more rigid clutch disc springs instead of torsional springs which are used in SMF application. The application of DMF will be examined in detail following part in this paper.

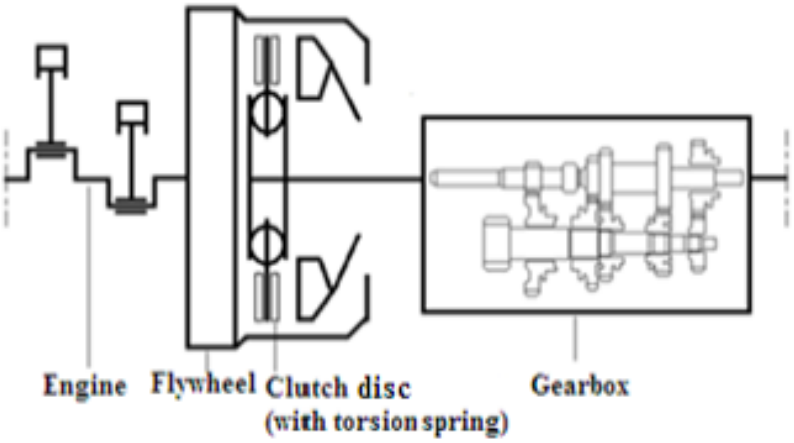

Figure 2.11: Power transmission system with SMF.

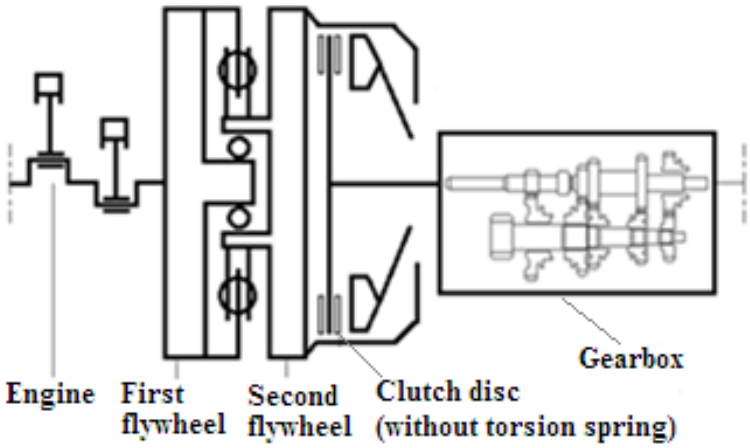

Figure 2.12: Power transmission system with DMF.

The comparison results of clutch dynamics with respect to used SMF and DMF is shown in Figure 2.13. For every gear, clutch engagement times are approximately same in SMF and DMF system. On the contrary, SMF speed oscillations after first contact are higher than DMF system. Absorb capability of DMF is better than

conventional system, and this shows that DMF application is smoother and more regular than SMF application. Besides, if the gears are compared within themselves, the engagement time increases as the gear increases.

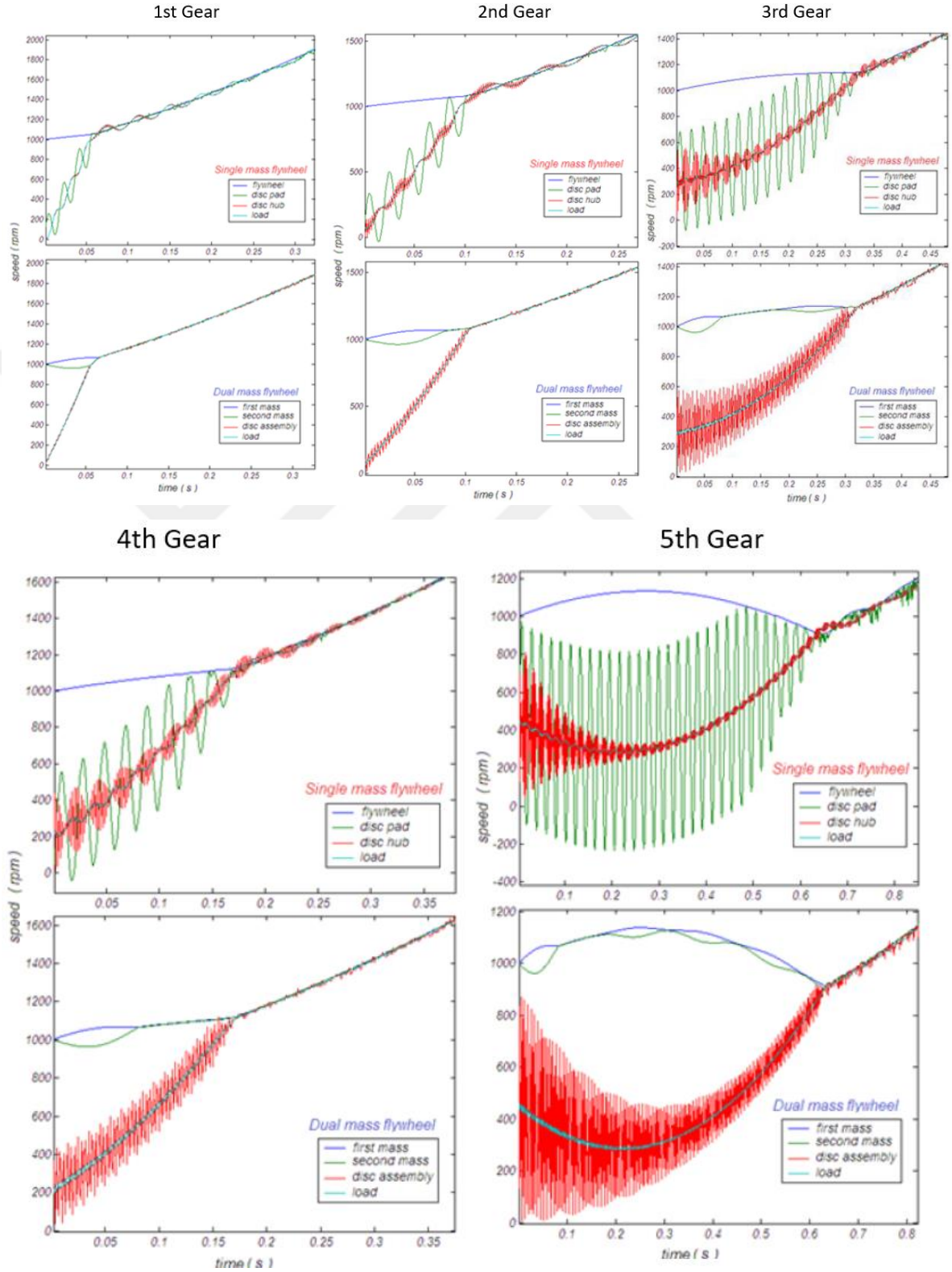

Figure 2.13: Compare clutch dynamic results in all gears (SMF / DMF).

As it is shown below Figure 2.14, the critical resonance frequency is reduced below the idle speed with using dual mass flywheel. While the red line represents system working with single mass flywheel, the blue line represents with dual mass flywheel in third gear.

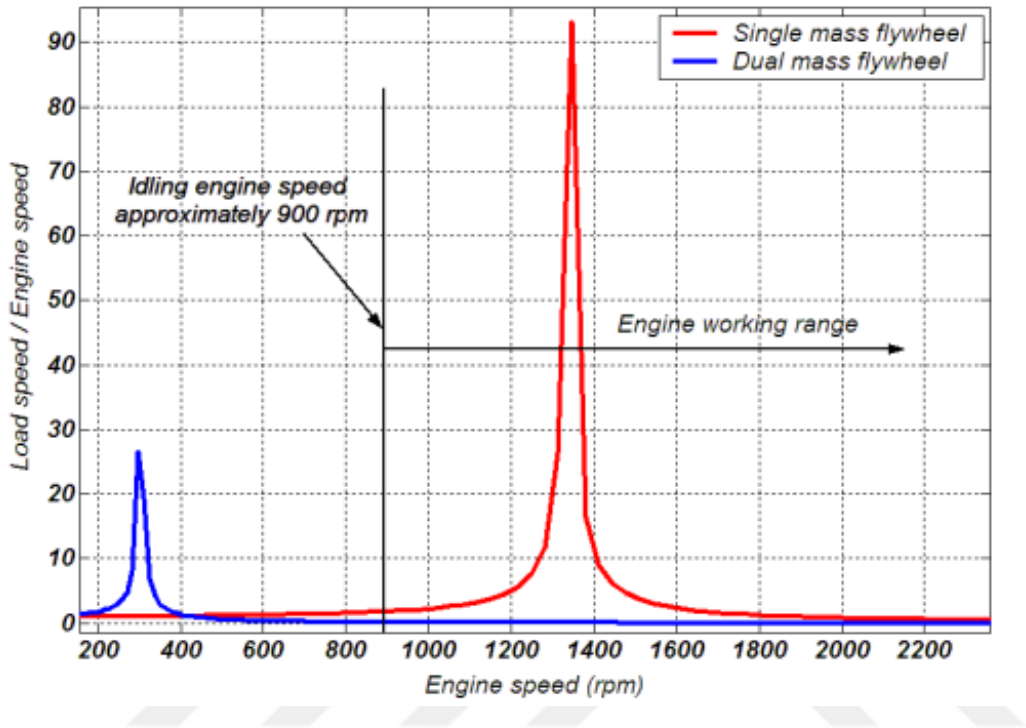

Figure 2.14: Compare to resonance characteristics of SMF and DMF system.

For different gear loads, the resonance characteristics of the SMF system are shown in Figure 2.15. Except fifth gear, whole gear resonance loads are in engine operation range with SMF system.

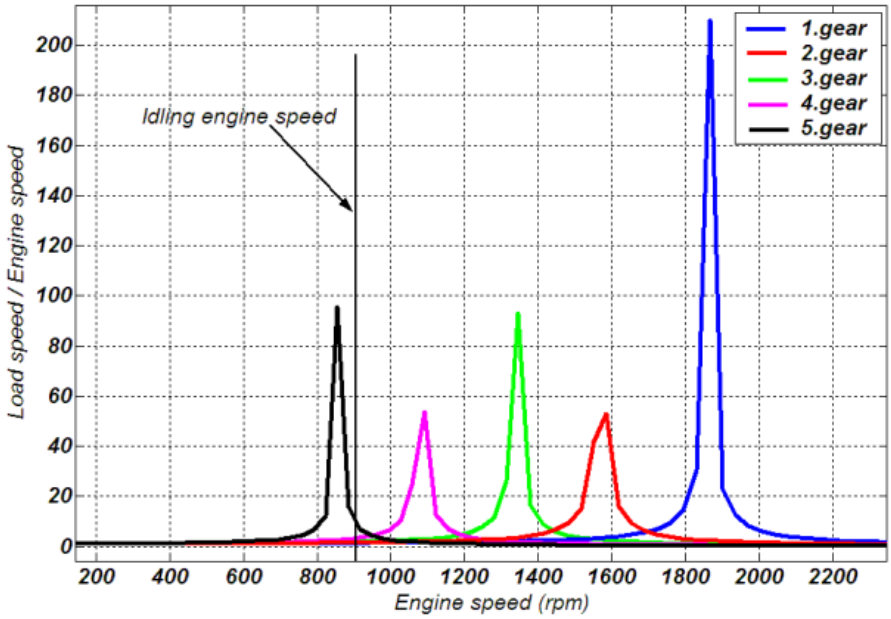

Figure 2.15: Resonance characteristic of SMF for all gear loads.

To prevent resonance during engine operation range, DMF system can be used. In Figure 2.16, resonance zones for whole gear loads are pull back to under the engine idle speed (under approximately 900rpm).

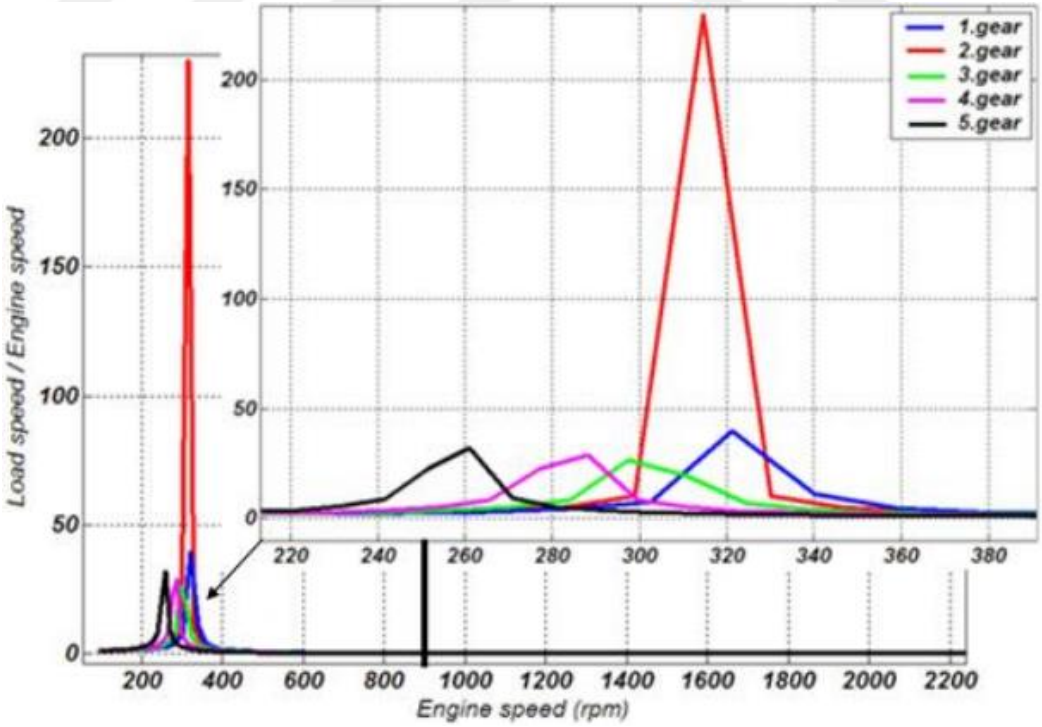

Figure 2.16: Resonance characteristic of DMF system for all gear loads.

3. MATHEMATICAL BACKGROUND

Dual mass flywheel is modelled as 2-DOF system and also DMF is connected to ICE and another side is transmission (gear) side. ICE side is considered as in-line 6-cylinder truck engine. Besides, engine torque is aforethought a sum of constant torque value and sine function.[5]

$$\boldsymbol{T_e(t) = T_0 + T_1(\sin(wt + \phi))} \tag{3.1}$$

In this paper, according to analysis data, $T_0 = 1600\ Nm$ and $T_1 = 200Nm$ Another assumption is that there are no vibrations at transmission side. [5]

When the equation of motion system can be easily solved with ODE45 Matlab function. The first order differential equations can be solved with ODE45, therefore, whole equations require to transforming from second order differential equations to first order differential equations in Matlab. In this way, θ_t matrix can be created like below;

$$\theta_t = \left[\theta_1, \dot{\theta_1}, \theta_2, \dot{\theta_2}\ \right]^T \tag{3.2}$$

And then, matrix can be modified as following,

$$\dot{\theta}_t = \left[\dot{\theta_1}, \ddot{\theta_1}, \dot{\theta_2}, \ddot{\theta_2}\ \right]^T = \left[\theta_t(2), \ddot{\theta_1}, \theta_t(4), \ddot{\theta_2}\ \right]^T \tag{3.3}$$

3.1 Time Domain

As shown in Figure 3.1, two damped harmonic oscillators are coupled with a non-linear elastic spring (k_{nl}). Oscillators have different mass (inertia), damping ratio (dissipative) and spring (elastic) properties.[2] This system with two oscillators has two degree of freedom and first oscillator is grounded on one end. Besides, second oscillator is free on the other end. As shown in Figure 3.1, this system is disturbed by external dynamic force which is applied on second mass.[1]

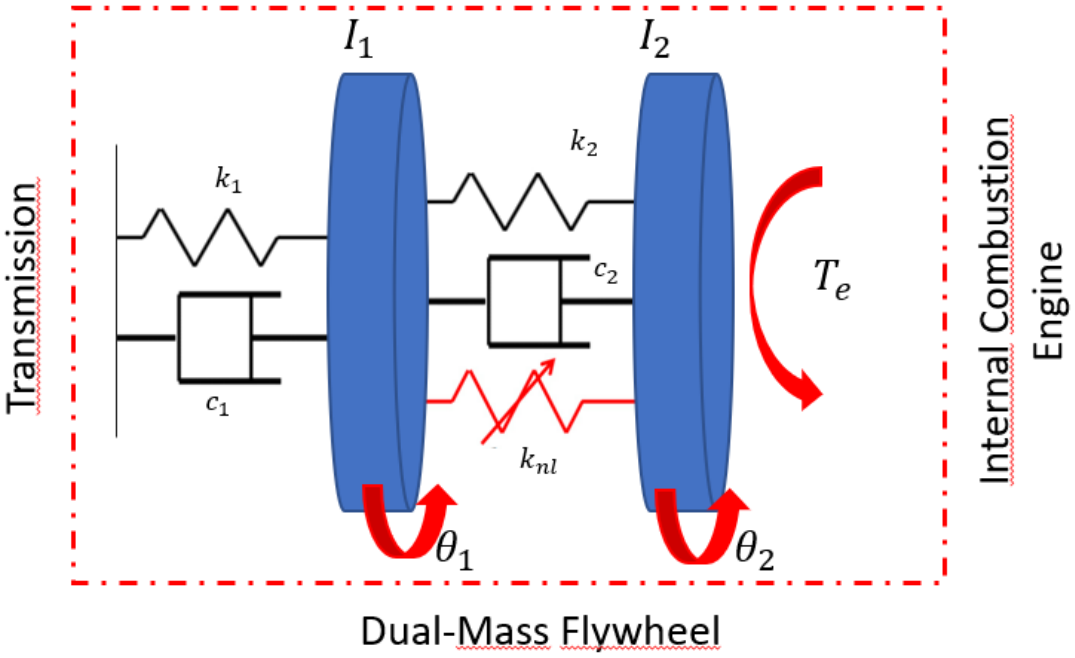

Figure 3.1: Scheme of DMF mathematical model.

The elastic path in non-linear system is assumed to present cubic non-linearity. Therefore, the non-linearity term should be cubic and as shown equation 1 and 2;

$$I_1\ddot{\theta}_1 + (c_1 + c_2)\dot{\theta}_1 - c_2\dot{\theta}_2 + (k_1 + k_2)\theta_1 - k_2\theta_2 - k_{nl}(\theta_2 - \theta_1)^3 = 0 \quad (3.4)$$

$$I_2\ddot{\theta}_2 + c_2\dot{\theta}_2 - c_2\dot{\theta}_1 + k_2\theta_2 - k_2\theta_1 + k_{nl}(\theta_2 - \theta_1)^3 = T_e(t) \quad (3.5)$$

In order to simplify above equations, non-dimensional parameters should be used;

$$w_n = \sqrt{\frac{k}{I}}, \qquad \zeta = \frac{c}{2Iw_n}, \qquad \tau = w_n t, \qquad \theta_0 = \frac{A}{k}$$

$$\theta_1 = \frac{\theta_1}{\theta_0}, \qquad \theta_2 = \frac{\theta_2}{\theta_0}, \qquad \alpha = \frac{k_{nl}\theta_0^2}{k_2}, \quad CR = \frac{c_2}{c_1}, \quad KR = \frac{k_2}{k_1}, \quad IR = \frac{I_2}{I_1}$$

The non-dimensional parameters are applied on governing equations as follows;

$$\theta_1'' + 2\zeta(1 + CR)\theta_1' - 2\zeta CR\theta_2' + (1 + KR)\theta_1 - KR\theta_2 - \alpha(\theta_2 - \theta_1)^3 = 0 \quad (3.6)$$

$$IR\theta_2'' + 2\zeta\theta_2' - 2\zeta\theta_1' + \theta_2 - \theta_1 + \alpha(\theta_2 - \theta_1)^3 = \sin(\frac{w}{w_{n_2}}\tau + \phi) \quad (3.7)$$

where $\theta_i' = \frac{d\theta_i}{d\tau}$ *and* $\theta_i'' = \frac{d^2\theta_i}{d\tau^2}$

According to the two equations extracted above, some cases are examined in the time domain and shown in the Section 4.

3.2 Frequency Domain

3.2.1 Nonlinear frequency responses using harmonic balance method

While steady-state response of non-linear system disturbing by a harmonic function non-linear system response is constructed, the multi-term harmonic balance method (MHBM) should be applied. $\Psi = \omega\tau$ is a linear independent variable transformation term and is used in order to ease the nonlinear governing equation formulation. In Ψ domain, nonlinear governing equations are following;

$$\omega^2 \frac{d^2\theta_1}{d\Psi^2} + 2\zeta(1+CR)\omega \frac{d\theta_1}{d\Psi} - 2\zeta CR\omega \frac{d\theta_2}{d\Psi} + (1+KR)\theta_1 - KR\theta_2 - \alpha(\theta_2-\theta_1)^3 = 0 \quad (3.8)$$

$$IR\omega^2 \frac{d^2\theta_2}{d\Psi^2} + 2\zeta\omega \frac{d\theta_2}{d\Psi} - 2\zeta\omega \frac{d\theta_1}{d\Psi} + \theta_2 - \theta_1 + \alpha(\theta_2-\theta_1)^3 = \sin(\frac{1}{\omega_n}\Psi + \emptyset) \quad (3.9)$$

θ_1 and θ_2 are considered in the forms of truncated Fourier series. N_h represents the number of harmonics retained.

$$\theta_1(\Psi) = a_{1,0} + \sum_{n=1}^{Nh} a_{1,2n-1}\sin(n\Psi) + a_{1,2n}\cos(n\Psi) \quad (3.10)$$

$$\theta_2(\Psi) = a_{2,0} + \sum_{n=1}^{Nh} a_{2,2n-1}\sin(n\Psi) + a_{2,2n}\cos(n\Psi) \quad (3.11)$$

θ_1 and θ_2 is also shown as $\theta_1 = \Gamma a_1$ and $\theta_2 = \Gamma a_2$ where Γ is the discrete Fourier transform matrix (DFTM).

a_1 = Unknown Fourier coefficient vectors of the dependent variable θ_1

a_2 = Unknown Fourier coefficient vectors of the dependent variable θ_2

The matrix Γ is defined as;

$$\Gamma = \begin{bmatrix} 1 & \sin(\Psi_0) & \cos(\Psi_0) & \cdots & \sin(N_h\Psi_0) & \cos(N_h\Psi_0) \\ 1 & \sin(\Psi_1) & \cos(\Psi_1) & \cdots & \sin(N_h\Psi_1) & \cos(N_h\Psi_1) \\ \vdots & \vdots & \vdots & \ddots & \vdots & \vdots \\ 1 & \sin(\Psi_{N-1}) & \cos(\Psi_{N-1}) & \cdots & \sin(N_h\Psi_{N-1}) & \cos(N_h\Psi_{N-1}) \end{bmatrix} \quad (3.12)$$

N : The number of discrete points

To protect from any aliasing problems, N is bigger than two times of N_h. The non-dimensional governing equations are as following;

$$\omega^2\Gamma D^2 a_1 + 2\zeta 1+CR)\omega\Gamma D a_1 - 2\zeta CR\omega\Gamma D a_2 + (1+KR)\Gamma a_1 - KR\Gamma a_2 - \alpha(\Gamma a_2 - \Gamma a_1)^3 = 0 \quad (3.13)$$

$$IR\omega^2\Gamma D^2 a_2 + 2\zeta\omega\Gamma D a_2 - 2\zeta\omega\Gamma D a_1 + \Gamma a_2 - \Gamma a_1 + \alpha(\Gamma a_2 - \Gamma a_1)^3 = \Gamma Q \quad (3.14)$$

D : Differential Operator

Q: Fourier coefficients vector for the external force excitation

$$D = \begin{bmatrix} 0 & 0 & 0 & \cdots & 0 & 0 \\ 0 & 0 & -1 & \cdots & 0 & 0 \\ 0 & 1 & 0 & \cdots & 0 & 0 \\ \vdots & \vdots & \vdots & \ddots & \vdots & \vdots \\ 0 & 0 & 0 & \cdots & 0 & -N_h \\ 0 & 0 & 0 & \cdots & N_h & 0 \end{bmatrix} \quad (3.15)$$

The unknowns, a_1 and a_2, are calculated by minimizing residue functions;

$$R_1 = \omega^2 D^2 a_1 + 2(\xi + M)\omega D a_1 - M\omega D a_2 + (1+R)a_1 - R a_2 - \alpha\Gamma^+(\Gamma a_2 - \Gamma a_1)^3 \ldots. (3.16)$$

$$R_2 = IR\omega^2 D^2 a_2 + 2\xi\omega D a_2 - 2\xi\omega D a_1 + a_2 - a_1 + \alpha\Gamma^+(\Gamma a_2 - \Gamma a_1)^3 - Q \quad (3.17)$$

Γ^+ : Pseudo-Inverse of the discrete Fourier transform matrix $\boldsymbol{(\Gamma^+ = (\Gamma^T\Gamma)^{-1}\Gamma^T)}$

With using Newton-Raphson iteratively, the residue minimization is applied. The vector of unknowns is as following;

$$\eta = [a_1 \quad a_2 \quad \omega]^T \quad (3.18)$$

The vector of residue is also as following;

$$R = [R_1 \quad R_2]^T \quad (3.19)$$

Iteration is applied in order to create Newton-Raphson scheme

$$\eta_{i+1} = \eta_i - J_i^{-1} R_i \quad (3.20)$$

Jacobian matrix, J, is defined as following;

$$J = \begin{bmatrix} \frac{\partial R_1}{\partial a_1} & \frac{\partial R_1}{\partial a_2} & \frac{\partial R_1}{\partial \omega} \\ \frac{\partial R_2}{\partial a_1} & \frac{\partial R_2}{\partial a_2} & \frac{\partial R_2}{\partial \omega} \end{bmatrix} \quad (3.21)$$

4. ANALYSIS AND RESULTS

4.1 System Analysis on Time Domain

Forth section in this paper, some parameters that be affected on system performance and characteristics will be analyzed. To analyze system, system initial parameters should be recognized. Dual mass flywheel system is represented by two springs which have stiffness characteristic of system, two dampers which have damper characteristic and two masses include main flywheel and secondary mass. Besides, one non-linear spring will perform in the system in order to create non-linear path.

In this section, the parameters listed below will be examined.

- I_2/I_1
- c_2/c_1
- k_1/k_2 , k_{nl}

The characteristics of the primary mass will be indicated by index 1, while the characteristics of the secondary flywheel will be indicated by index 2.

In vehicle industry, some powertrain manufacturers use dual mass flywheel to increase the transmission system life. In Table 4.1, the following values have been accepted according to the benchmark data examined.[Url-1][12]

Table 4.1: Initial parameters of DMF.

Parameter	Unit	Value
Inertia of primary flywheel	$I_1\ (kgm^2)$	0.130
Inertia of secondary mass	$I_2\ (kgm^2)$	0.065
The damping factor between transmission - flywheel	$c_1\ \left(\frac{Ns}{m}\right)$	0.4
The damping factor between flywheel - engine	$c_2\ \left(\frac{Ns}{m}\right)$	0.1
The spring coefficient between transmission - flywheel	$k_1\ \left(\frac{Nm}{deg}\right)$	600
The spring coefficient between flywheel - engine	$k_2\ \left(\frac{Nm}{deg}\right)$	300
The non-linearity characteristic	α	0.02
Main torque value	$T_0\ (Nm)$	1600
Oscillation torque value	$T_1\ (Nm)$	200
Frequency of external torque (Engine speed)	$\omega\ (Hz)$	20

While preparing this mathematical model, the engine and transmission sides have been simplified to reduce complexity and the system has 2 degrees of freedom. At this point, it is seen that the vibrations on the engine side vary, but the vibrations on the transmission side have a constant profile. Therefore, the transmission side is kept constant, and the torque effect is given by the internal combustion engine. The effect of the ICE side, which is also shown in Figure 3.1, is combined with the main mass. On the other side of the model, the transmission side is kept constant. In the results, the displacement of the primary mass will be seen as the reaction force on the flywheel, while the displacement of the secondary mass will show the amount transferred to the transmission. Accordingly, we expect θ_1 values to be smaller than θ_2 values.

In Figure 4.1, the first parameters show the displacement of the primary and secondary masses. In the following sub-headings, the situations obtained with the changed parameters will be compared with the situation obtained with the initial values here.

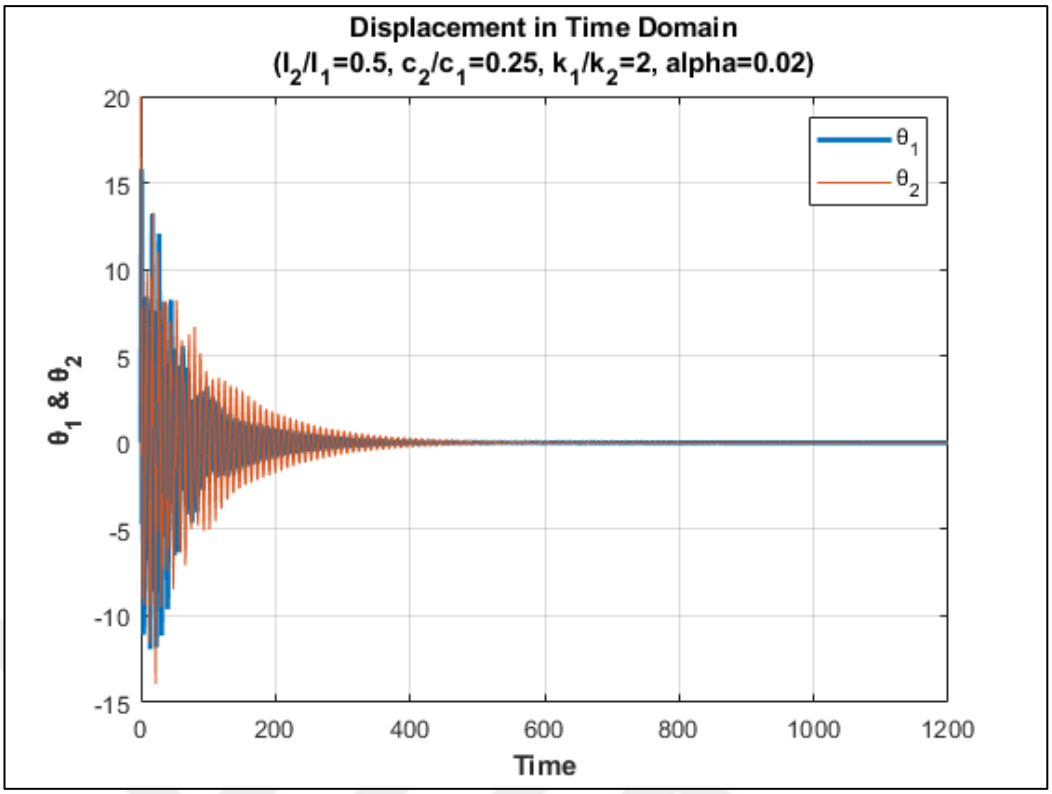

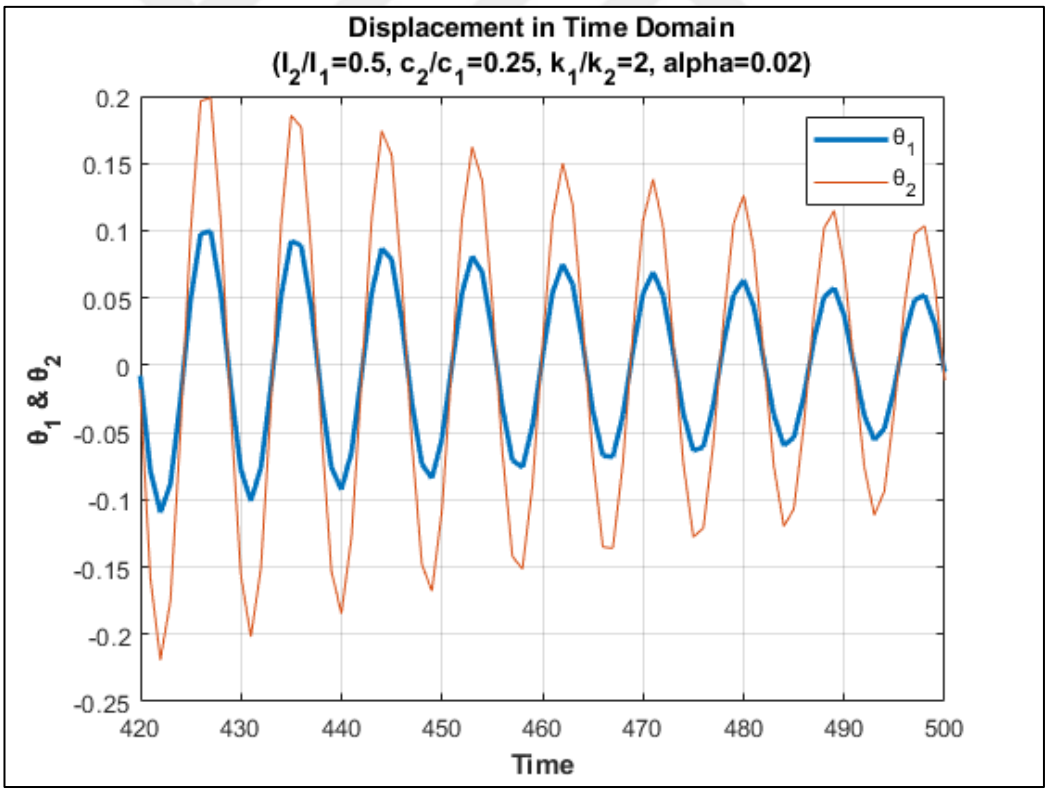

Figure 4.1: Displacement in time domain (initial situation: (a)full-scale (b)zoomed).

4.1.1 The inertia ratio effect (I_2/I_1)

4.1.1.1 Higher inertia ratio

The inertia of first and second masses are set to 0.135 kgm^2 and 0.095 kgm^2 respectively. When the mass ratio I_2/I_1 is equal to 0.731, the displacements of mass are shown in time domain in Figure 4.2;

- Response time will decrease
- Displacement of primary mass will increase (I_1 $constant$)
- Displacement of secondary mass will increase (I_2 $increases$)

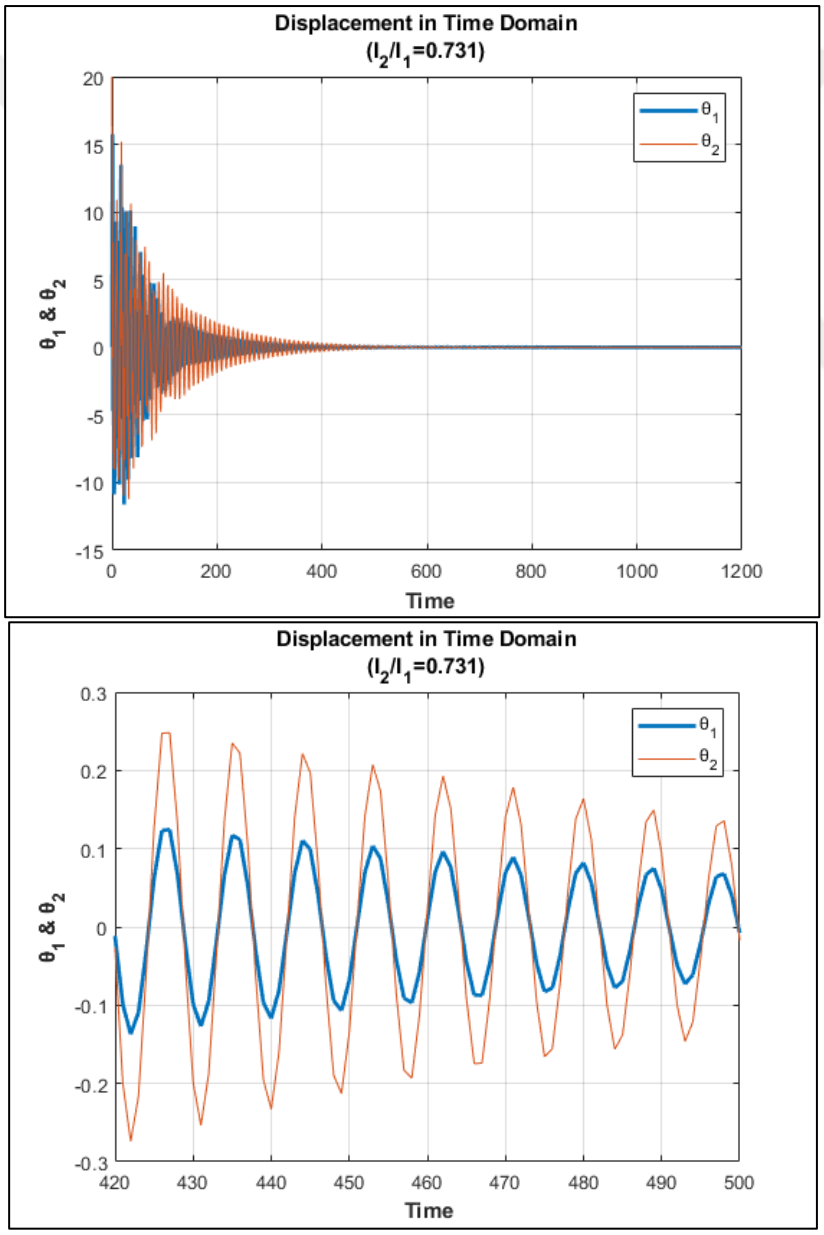

Figure 4.2: Displacement in time domain (I_2/I_1=0.731) (a)full-scale (b)zoomed.

4.1.1.2 Lower inertia ratio

The inertia of first and second masses are set to 0.135kgm^2 and 0.030kgm^2 respectively. When the mass ratio I_2/I_1 is equal to 0.231, the displacements of mass are shown in time domain in Figure 4.3;

- Response time will decrease
- Displacement of primary mass will decrease (I_1 $constant$).
- Displacement of secondary mass will decrease (I_2 $decreases$)

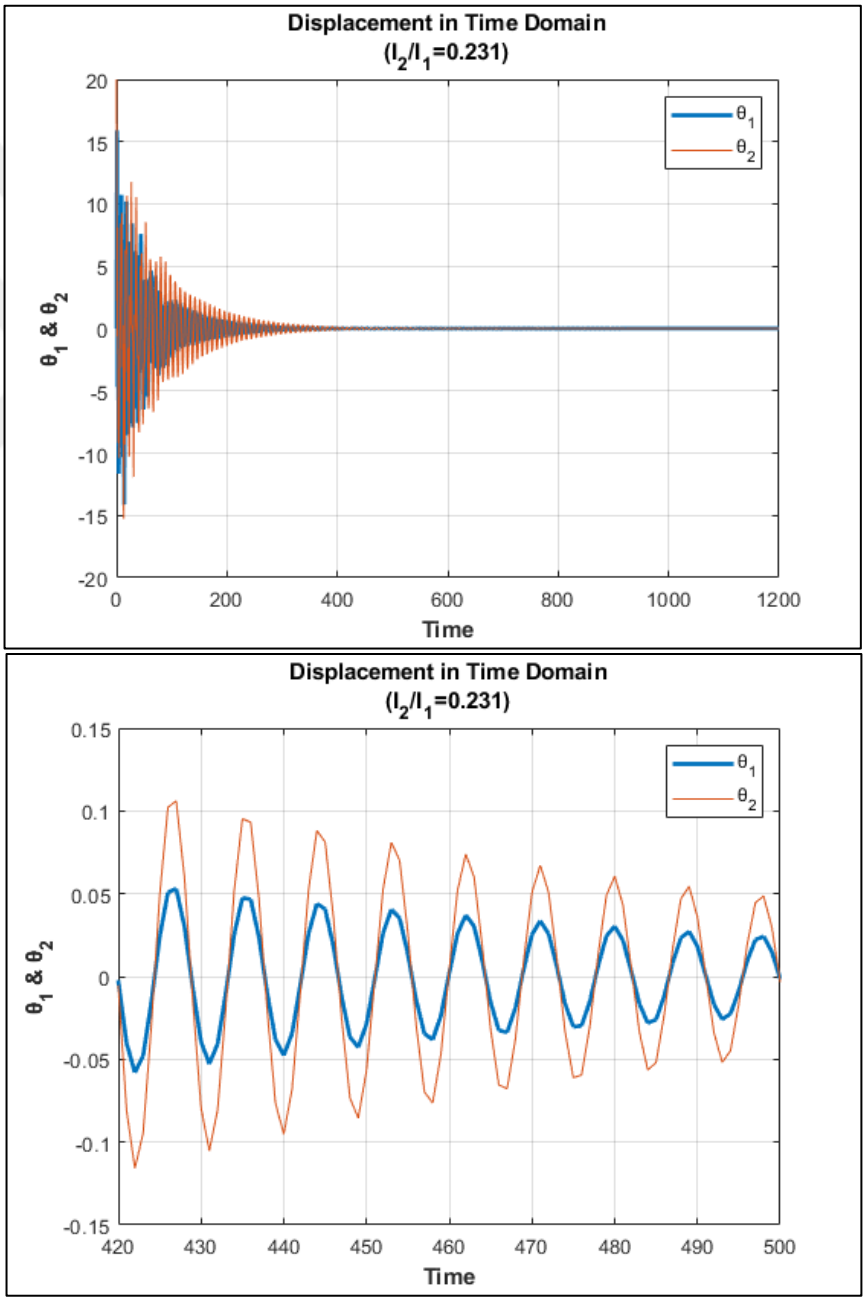

Figure 4.3: Displacement in time domain (I_2/I_1=0.231) (a)full-scale (b)zoomed.

To understand clearly, system inertia modifications and their effects are shown in below Table 4.2;

Table 4.2: The inertia ratio effect on $\boldsymbol{\theta_1}$ and $\boldsymbol{\theta_2}$ displacements.

Case Number	$\mathbf{I_2/I_1}$	$\boldsymbol{\theta_1}$	$\boldsymbol{\theta_2}$	Stable Response Time [s]
0	0.5	+/-0.069	+/-0.162	469
1	0.731	0.089/-0.083	0.207/-0.193	542
2	0.231	0.033/-0.030	0.081/-0.076	435

The first important parameter of the system is inertia ratio. In this comparison, main flywheel body is kept constant, and all changes are applied on secondary mass. Dual mass can be choosing a material which has less or more inertia.

In first case, secondary mass has more inertia as initial condition, that means inertia ratio (I_2/I_1) is high with respect to initial condition, main flywheel and secondary body displacement will increase, but the spending time to stabilize main flywheel body is longer than initial condition. The displacements of both mass increase approximately 25%.

Another variation is that secondary mass (I_1) can be had less inertia as initial condition. In this case, inertia ratio (I_2/I_1) is low, main flywheel and secondary body displacement will decrease. Besides, the spending time to stabilize main flywheel body is less than first case. The displacements of both mass decrease approximately 50%.

When the inertia of the mass on the transmission side (secondary mass) has a higher value, the stabilization time of the system increases around 15%. On the contrary, the stabilization time of the system decreases around 7% if the secondary mass has lower inertia value.

4.1.2 The damping factor ratio effect (c_2/c_1)

4.1.2.1 Higher damping factor ratio

The first and second dampers are set to 0.4 Ns/m and 0.2 Ns/m respectively. When the damping factor ratio c_2/c_1 is equal to 0.5, the displacements of mass are shown in time domain in Figure 4.4;

- Response time will decrease
- Displacement of primary mass will decrease (c_1 $constant$)
- Displacement of secondary mass will decrease (c_2 $increases$)

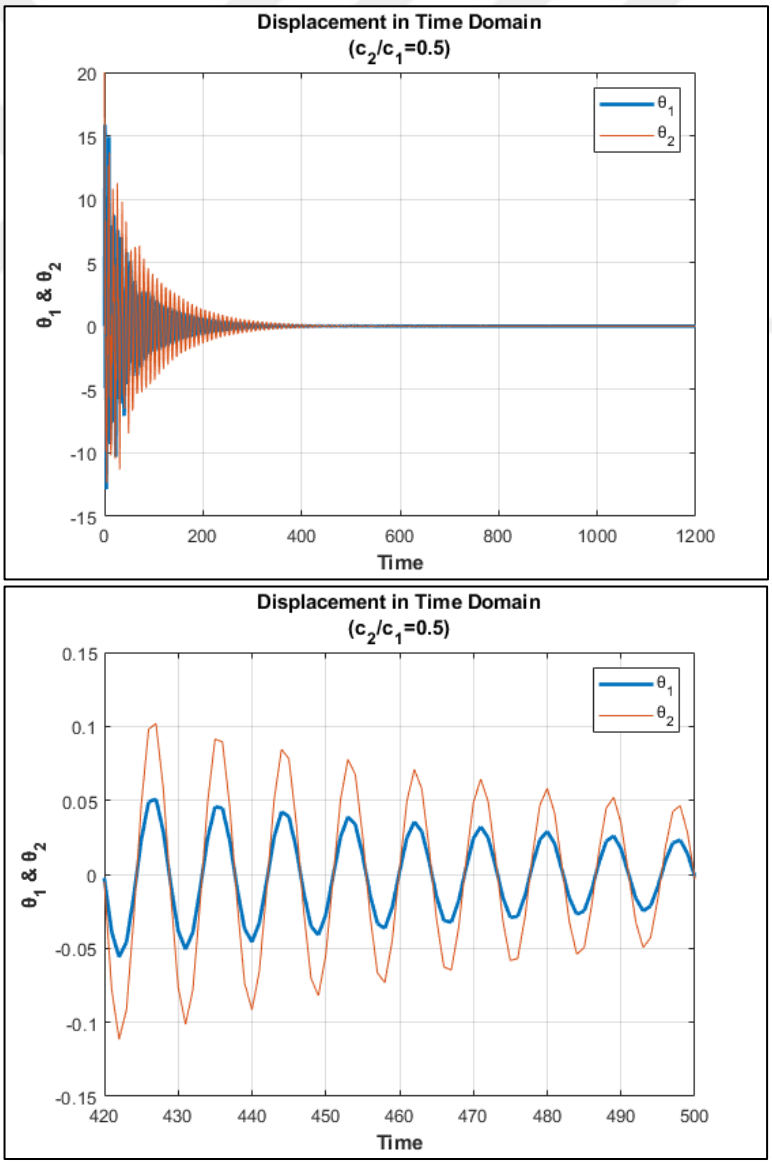

Figure 4.4: Displacement in time domain (c_2/c_1=0.5) (a)full-scale (b)zoomed.

4.1.2.2 Lower damping factor ratio

The first and second dampers are set to 0.4 Ns/m and 0.05 Ns/m respectively. When the damping factor ratio c_2/c_1 is equal to 0.125, the displacements of mass are shown in time domain in Figure 4.5;

- Response time will increase
- Displacement of primary mass will increase (c_1 $constant$)
- Displacement of secondary mass will increase (c_2 $decreases$)

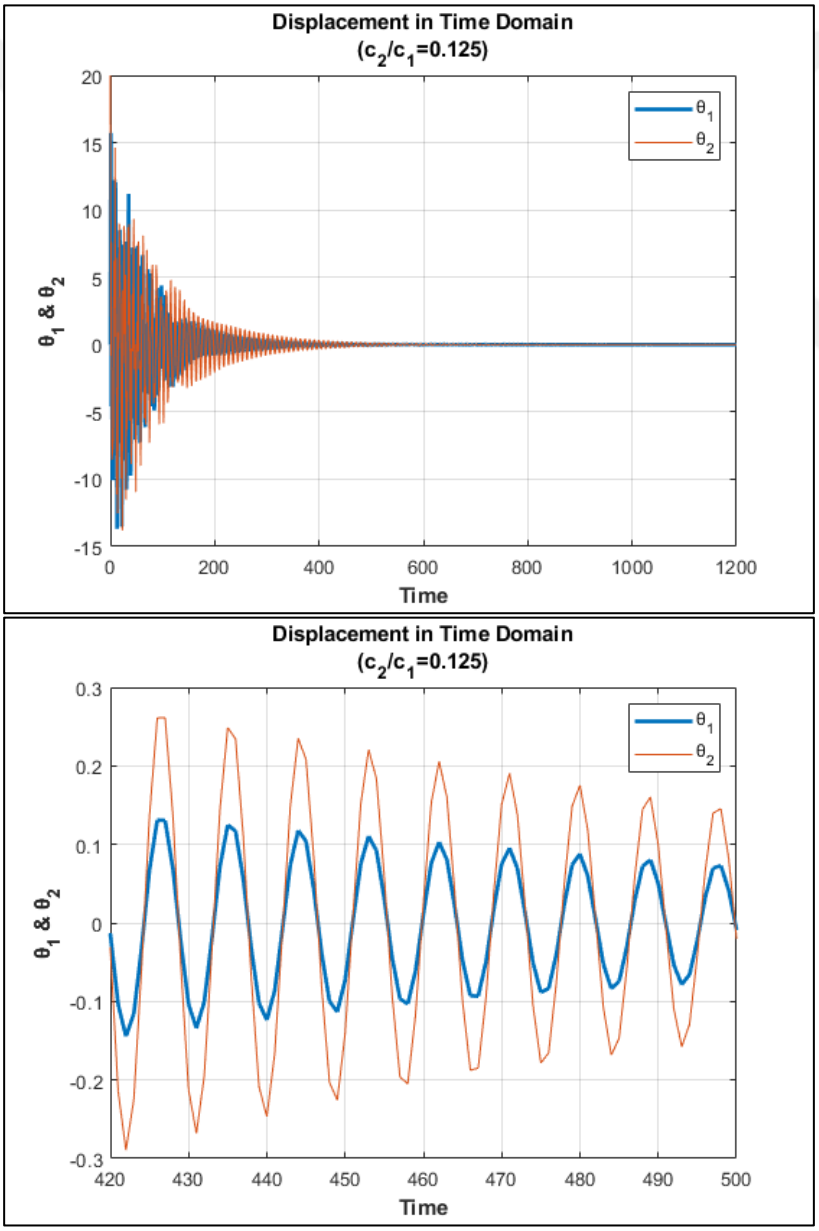

Figure 4.5: Displacement in time domain (c_2/c_1=0.125) (a)full-scale (b)zoomed.

To understand clearly, system damping modifications and their effects are shown in below Table 4.3;

Table 4.3: The damping ratio effect on $\boldsymbol{\theta_1}$ and $\boldsymbol{\theta_2}$ displacements.

Test Number	c_2/c_1	θ_1	θ_2	Stable Response Time [s]
0	0.25	+/-0.069	+/-0.162	469
1	0.5	0.032/-0.029	0.078/-0.073	435
2	0.125	0.095/-0.088	0.221/-0.205	551

The second important parameter of the system is damping ratio. In this comparison, main flywheel body is kept constant, and all changes are applied on secondary mass. Dual mass can be chosen a material which has less or more damping performance.

In first case, damping ratio is high, main flywheel and secondary body displacement will decrease, and the spending time to stabilize main flywheel body is less than initial conditions. The increment of displacement is about 55%.

Secondary mass can be used in less damped material as second case. In this case, damping ratio is low, main flywheel and secondary body displacement will increase. Besides, the spending time to stabilize main flywheel body is longer than initial and first case. The displacements of both mass decrease 32% according to initial case.

When the damping coefficient of the secondary mass on the transmission side has a higher value, the stabilization time of the system decreases around 7%. On the contrary, the stabilization time of the system increases around 17% if the secondary mass has lower damping coefficient.

4.1.3 The stiffness ratio effect (k_1/k_2)

4.1.3.1 Higher stiffness ratio

The first and second stiffness ratios are set to 600 Ns/m and 150 Ns/m respectively. When the damping factor ratio k_1/k_2 is equal to 4, the displacements of mass are shown in time domain in Figure 4.6;

- Response time will decrease
- Displacement of primary mass will decrease ($k_1\ constant$)
- Displacement of secondary mass will decrease ($k_2\ decreases$)

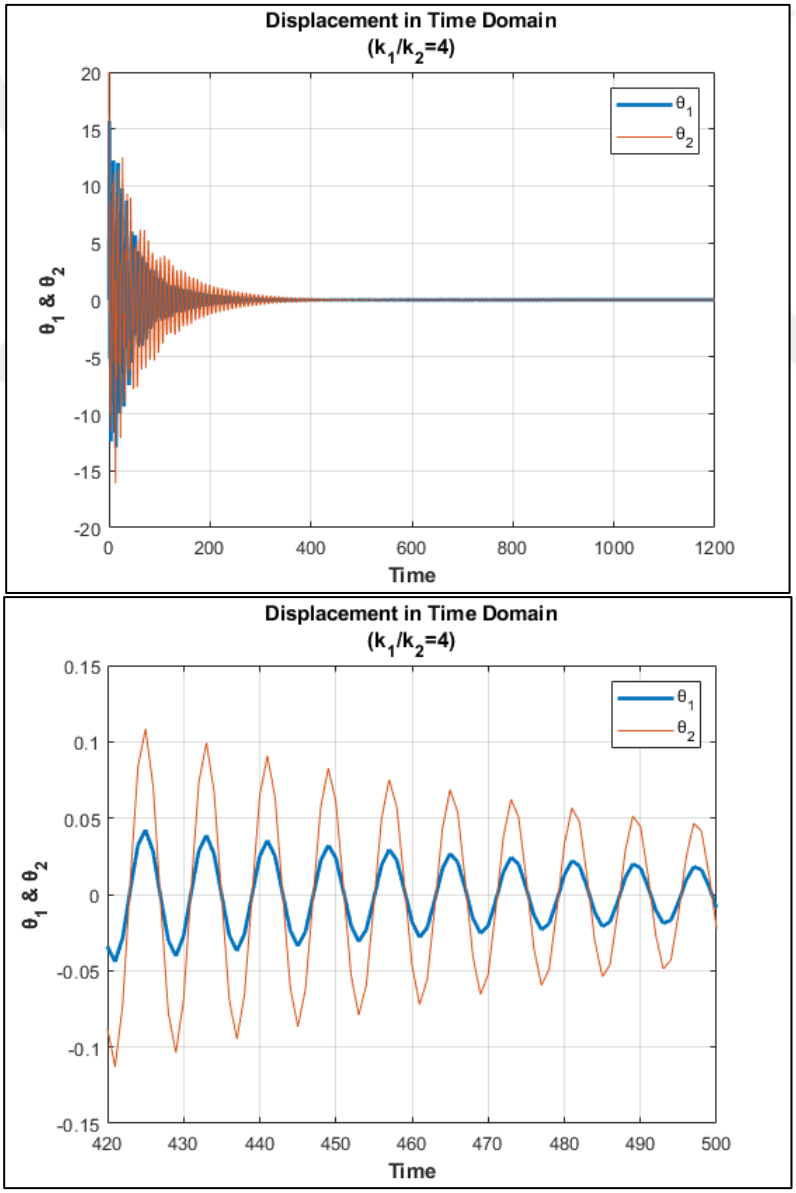

Figure 4.6: Displacement in time domain (k_1/k_2=4) (a)full-scale (b)zoomed.

4.1.3.2 Lower stiffness ratio

The first and second stiffness ratios are set to 600 Ns/m and 450 Ns/m respectively. When the damping factor ratio k_1/k_2 is equal to 1.3, the displacements of mass are shown in time domain in Figure 4.7;

- Response time will increase
- Displacement of primary mass will increase ($k_1\ constant$)
- Displacement of secondary mass will increase ($k_2\ increases$)

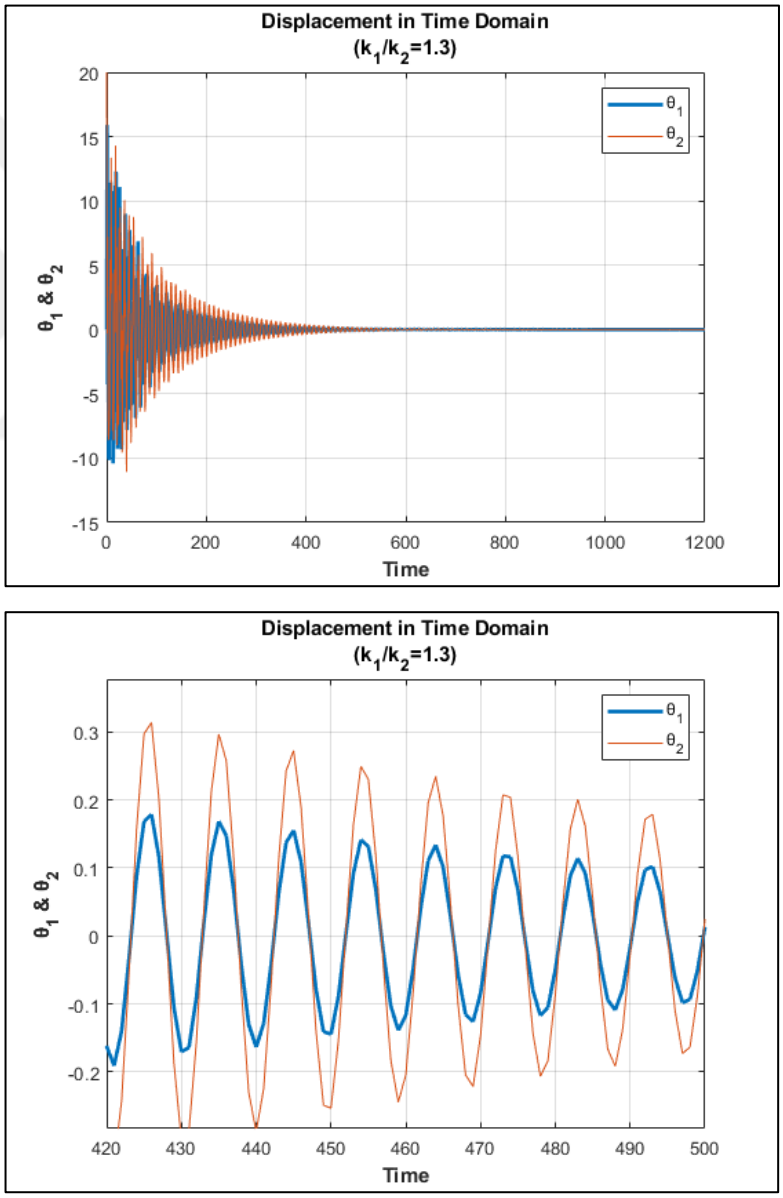

Figure 4.7: Displacement in time domain (k_1/k_2=1.3) (a)full-scale (b)zoomed.

To understand clearly, system stiffness modifications and their effects are shown in below Table 4.4;

Table 4.4: The stiffness ratio effect on $\boldsymbol{\theta_1}$ and $\boldsymbol{\theta_2}$ displacements.

Test Number	k_1/k_2	θ_1	θ_2	Stable Response Time [s]
0	2	+/-0.069	+/-0.162	469
1	4	+/-0.117	+/-0.250	569
2	1.3	0.024/-0.023	0.083/-0.079	441

The second important parameter of the system is stiffness ratio. In this comparison, ICE side is kept constant, and all changes are applied on transmission side. Thus, secondary stiffness coefficient can be chosen as a have less or more stiff material.

In first case, stiffness ratio is high, main flywheel displacement will increase, likewise, the displacement of secondary mass will also increase. Furthermore, the spending time to stabilize main flywheel body is longer than initial conditions. When the stiffness ratio increases, the displacement of primary mass increases by approximately 74%, the displacement of secondary mass increases by 50%.

Secondary mass can be used in more stiff material as second case. In this case, stiffness ratio (k_1/k_2) is low, primary and secondary body displacements will decrease. Besides, the spending time to stabilize main flywheel body is less than initial and first case. When the stiffness ratio decreases, the displacement of primary mass decreases by approximately 65%, the displacement of secondary mass increases by 50%.

The conclusion that can be drawn from here is that if more vibration comes from the engine, the vibration transmitted to the transmission side can be kept constant by reducing the spring stiffness coefficient of the main mass. On the contrary, if the engine vibration is low, the system can be operated with a high spring stiffness coefficient.

4.1.4 The non-linear stiffness ratio effect (α)

4.1.4.1 Higher non-linear stiffness ratio

The non-linear stiffness ratio is set to 0.5, the displacements of mass are shown in time domain in Figure 4.8;

- Response time will increase
- Displacement of primary mass will decrease
- Displacement of secondary mass will decrease

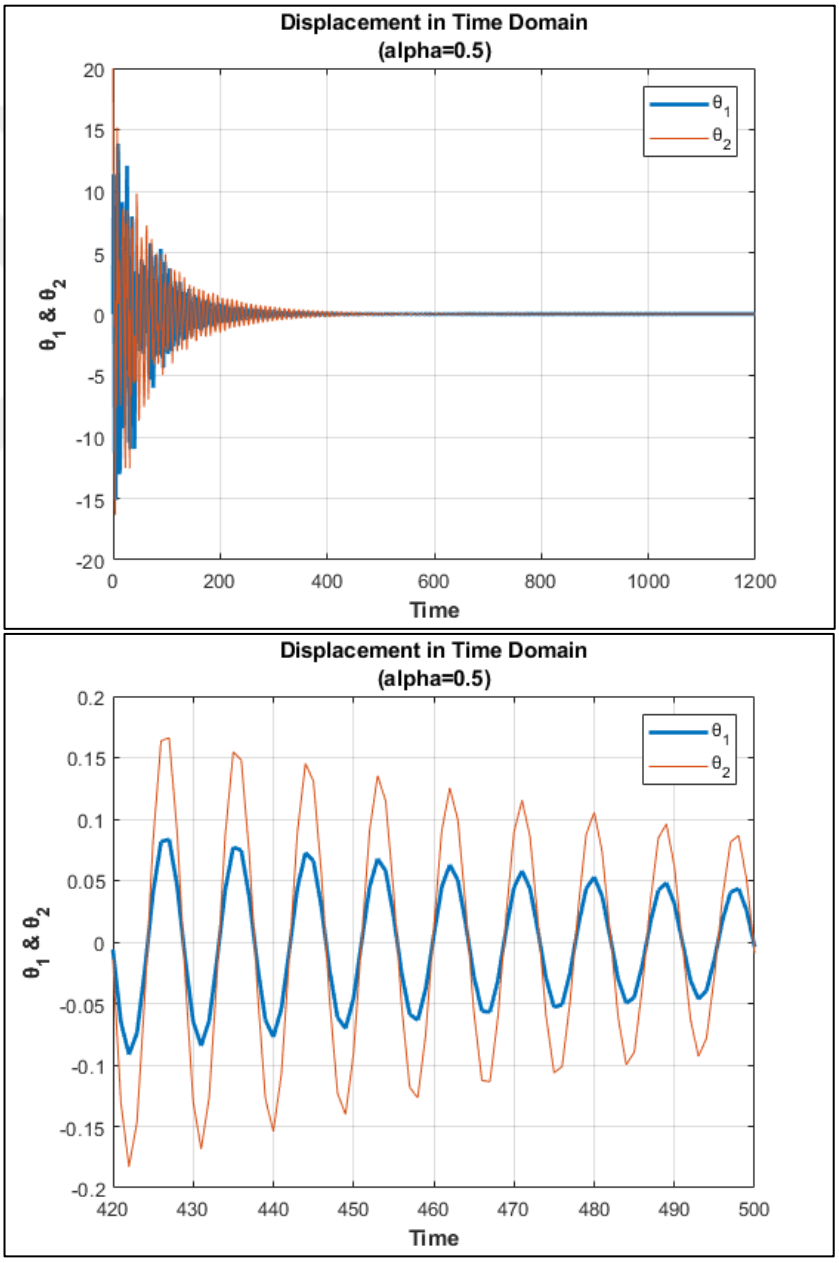

Figure 4.8: Displacement in time domain (α_1=0.5) (a)full-scale (b)zoomed.

4.1.4.2 Lower non-linear stiffness ratio

The non-linear stiffness ratio is set to 0.01, the displacements of mass are shown in time domain in Figure 4.9;

- Response time will increase
- Displacement of primary mass will increase
- Displacement of secondary mass will increase

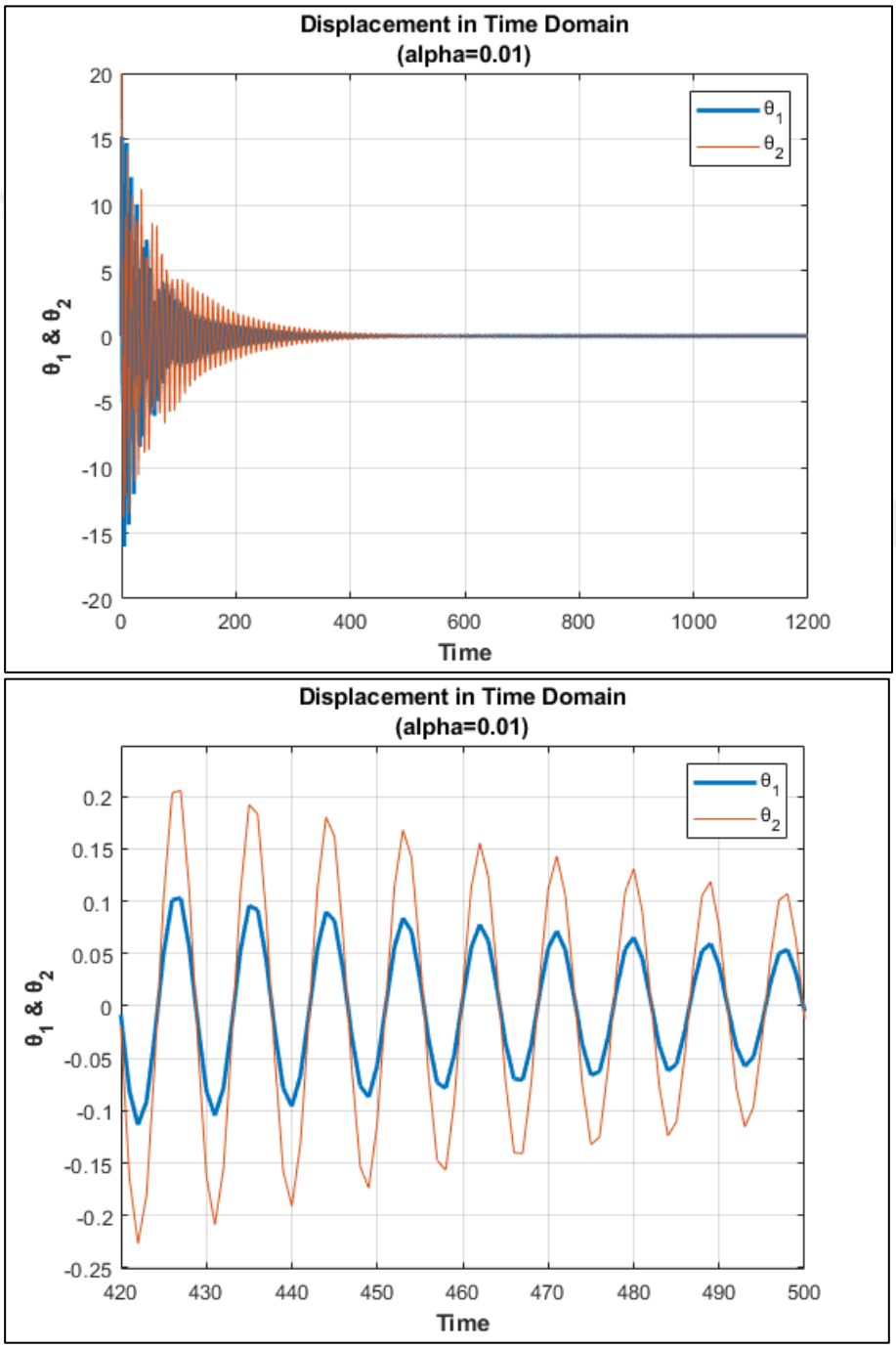

Figure 4.9: Displacement in time domain (α=0.01) (a)full-scale (b)zoomed.

4.1.4.3 Zero non-linear stiffness ratio

The non-linear stiffness ratio is set to 0, the displacements of mass are shown in time domain in Figure 4.10;

- Peak frequency will increase
- Displacement of primary mass will increase
- Displacement of secondary mass will increase

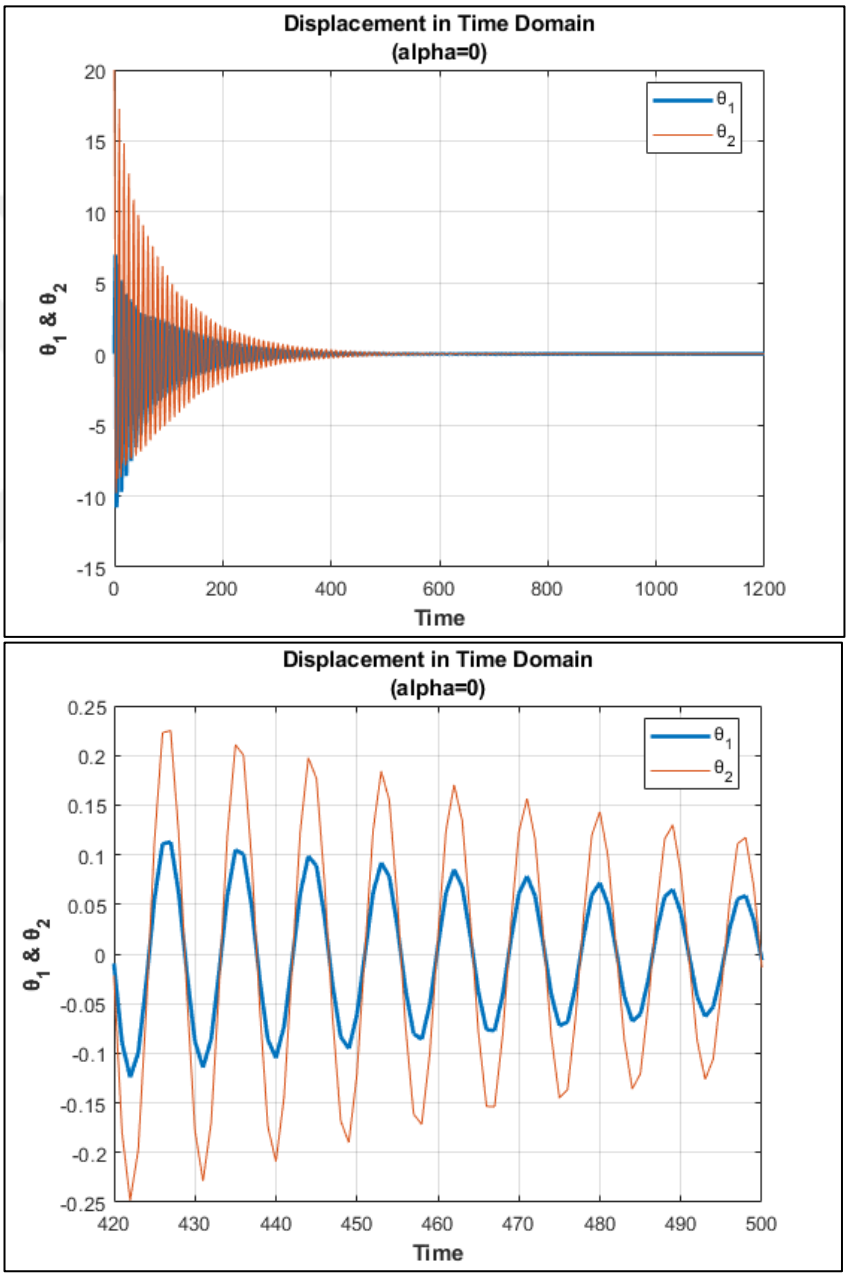

Figure 4.10: Displacement in time domain (α =0) (a)full-scale (b)zoomed.

To understand clearly, system stiffness modifications and their effects are shown in below Table 4.5;

Table 4.5: The non-linear stiffness ratio effect on $\boldsymbol{\theta_1}$ and $\boldsymbol{\theta_2}$ displacements.

Test Number	α	θ_1	θ_2	Stable Response Time [s]
0	0.02	+/-0.069	+/-0.162	469
1	0.5	0.057/-0.053	0.135/-0.127	489
2	0.01	0.072/-0.066	0.168/-0.157	507
3	0	0.078/-0.072	0.184/-0.171	524

Another important parameter of the system is non-linear stiffness ratio. For the first case, non-linear ratio is considered as 0.5 which means higher non-linear stiffness coefficient than initial case. In this case, displacements of both mass decrease. The displacements of primary and secondary mass decrease approximately 20%. Moreover, the spending time to stabilize system is increased.

For the second case, non-linear stiffness ratio is considered as 0.01 which means lower non-linear stiffness coefficient than initial case. For this case, displacements of both masses slightly increase. Primary and secondary masses displace 5% more according to initial case. Furthermore, the stable response time increases.

For linear situation which means alpha equal to zero, the displacements of both mass increase approximately 10%. Also, the stable response time increase around 12%.

4.2 System analysis on frequency domain

In this section, the parameters that affect to primary and secondary mass displacements are manipulated in frequency domain as being examined in time domain before.

In Figure 4.11, the displacements of the primary and secondary masses are showed with initial conditions. In the following sub-headings, the situations obtained with the changed parameters will be compared with the situation obtained with the initial values here.

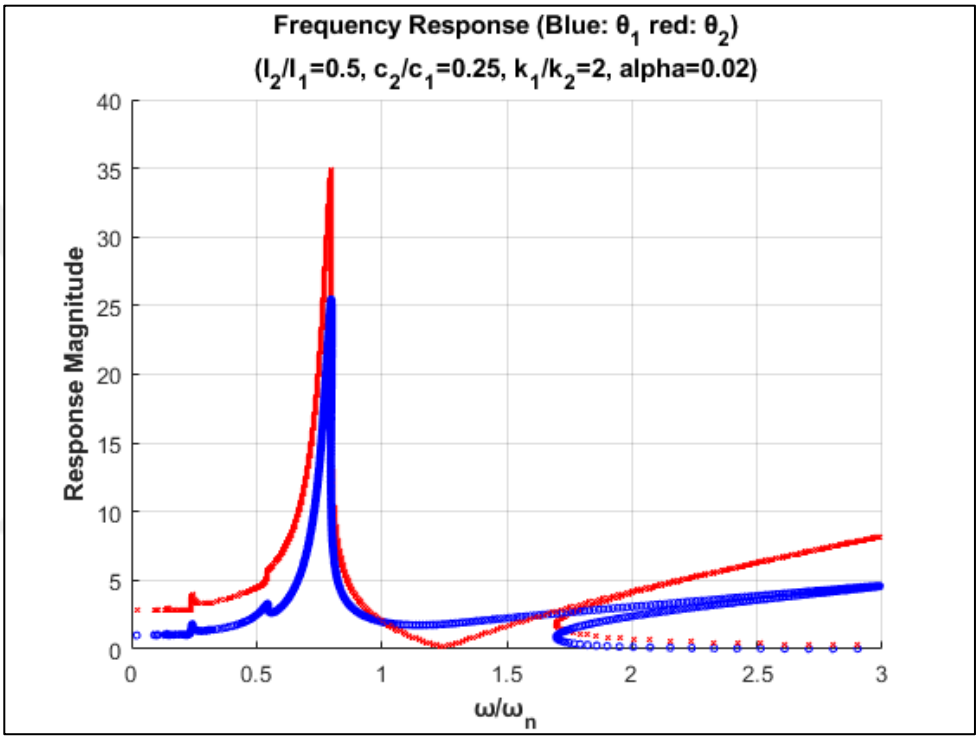

Figure 4.11: Displacement in frequency domain (initial case).

4.2.1 The inertia ratio effect (I_2/I_1)

4.2.1.1 Higher inertia ratio

The inertia of first and second masses are set to 0.130 kgm^2 and 0.095 kgm^2 respectively. When the mass ratio I_2/I_1 is equal to 0.731, the response magnitudes of mass are shown in time domain in Figure 4.12;

- Displacement of primary mass will increase (I_1 $constant$)
- Displacement of secondary mass will increase (I_2 $increases$)

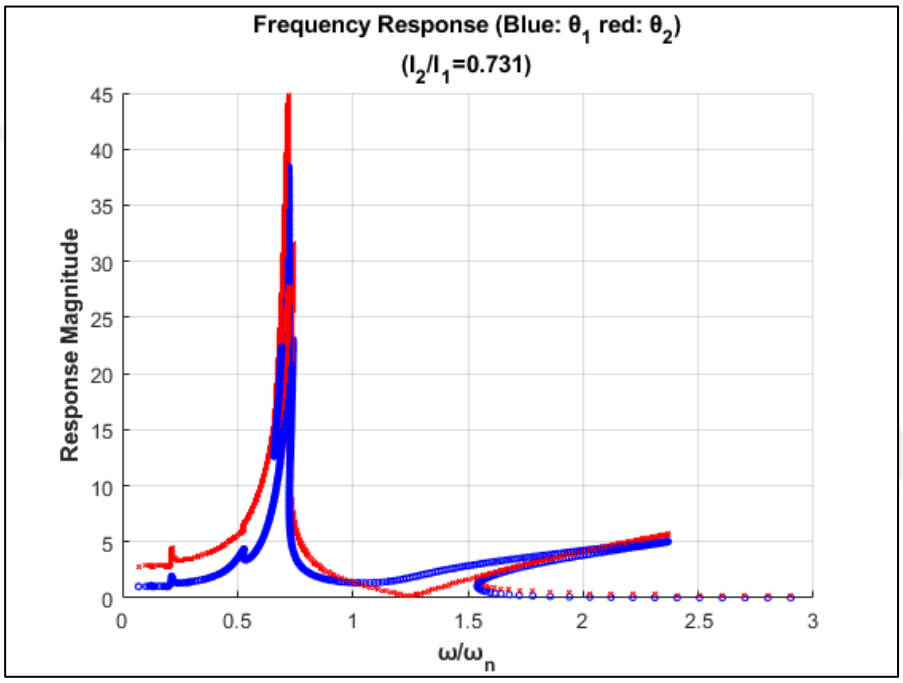

Figure 4.12: Displacement in frequency domain (I_2/I_1=0.731).

4.2.1.2 Lower inertia ratio

The inertia of first and second masses are set to 0.130kgm^2 and 0.030kgm^2 respectively. When the mass ratio I_2/I_1 is equal to 0.231, the response magnitudes of mass are shown in time domain in Figure 4.13;

- Displacement of primary mass will increase (I_1 $constant$).
- Displacement of secondary mass will slightly decrease (I_2 $decrease$)

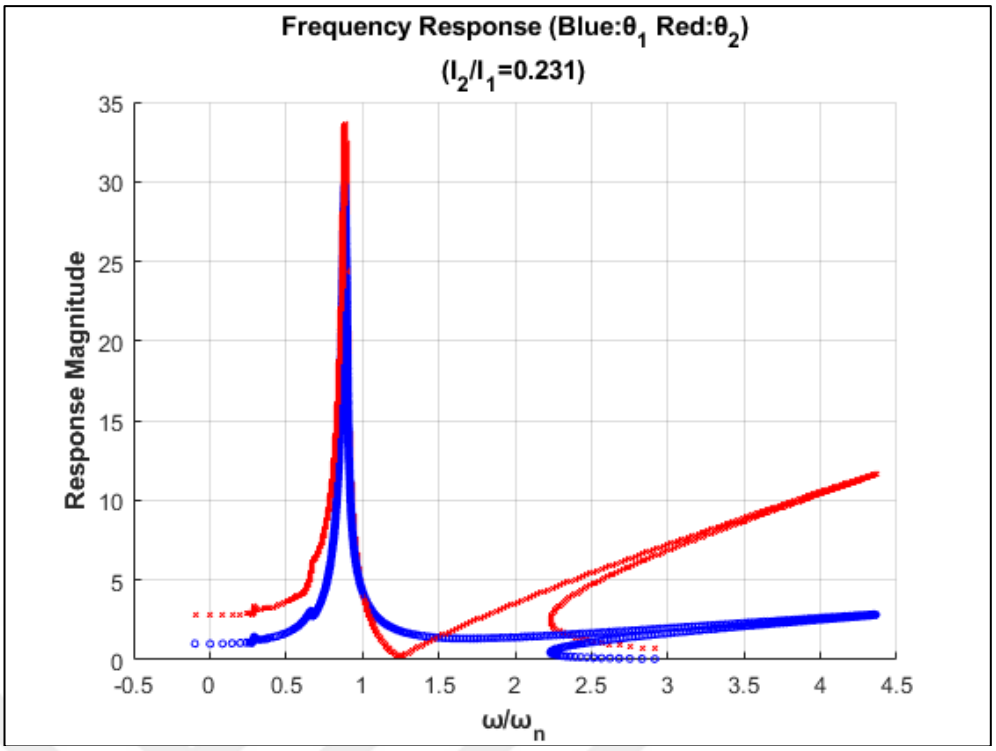

Figure 4.13: Displacement in frequency domain (I_2/I_1=0.231).

To understand clearly, system inertia modifications and their effects are shown in below Table 4.6;

Table 4.6: The inertia ratio effect on $\boldsymbol{\theta_1}$ and $\boldsymbol{\theta_2}$ displacements.

Test Number	I_2/I_1	θ_1	θ_2	Peak Frequency
0	0.5	25.453	34.868	0.799
1	0.731	38.457	44.730	0.722
2	0.231	29.796	33.579	0.884

The first important parameter of the system is inertia ratio. In this comparison, main flywheel body is kept constant, and all changes are applied on secondary mass. Dual mass can be choosing a material which has less or more inertia.

In first case, secondary mass (I_2) has more inertia as initial condition, that means inertia ratio (I_2/I_1) is high with respect to initial condition. While main flywheel displacement will increase 51%, secondary mass displacement will increase approximately 28%. Also, peak frequency will be shifted to 10% lower amplitude.

Another variation is that secondary mass (I_2) can be had less inertia as initial condition. In this case, inertia ratio (I_2/I_1) is low, main flywheel displacement will increase 17%. But secondary body displacement will slightly decrease about 4%. Besides, peak frequency will be shifted to 10% higher amplitude.

The inertia of secondary mass has crucial effect on response magnitude around 2nd natural frequency. While inertia increase, the response magnitude of both mass decrease around 2nd natural frequency. In contrast, when secondary mass has lower inertia value, the magnitudes increase around 2nd natural frequency. In addition, 2nd natural frequency value increases as inertia decreases.

4.2.2 The damping factor ratio effect (c_2/c_1)

4.2.2.1 Higher damping factor ratio

The first and second dampers are set to 0.4 Ns/m and 0.2Ns/m respectively. When the damping factor ratio c_2/c_1 is equal to 0.5, the response magnitudes of mass are shown in time domain in Figure 4.14;

- Displacement of primary mass will decrease ($c_1\ constant$)
- Displacement of secondary mass will be decrease ($c_2\ increase$)

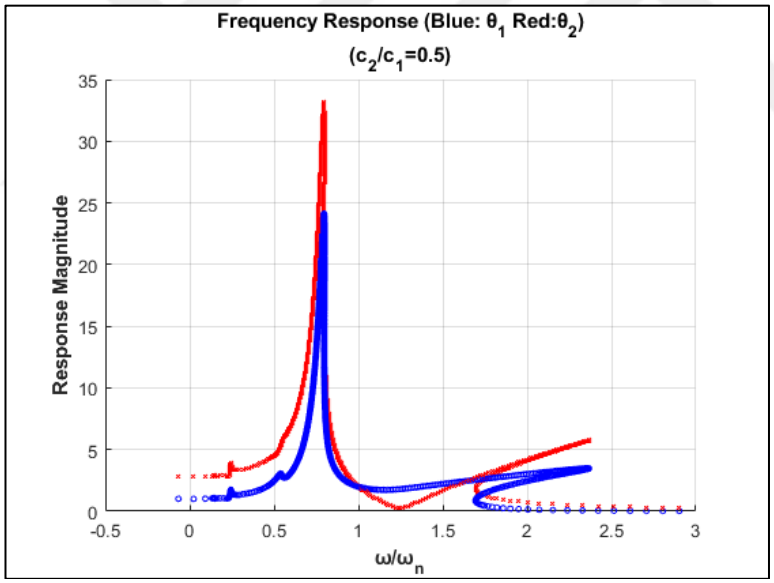

Figure 4.14: Displacement in time domain (c_2/c_1=0.5) (a)full-scale (b)zoomed.

4.2.2.2 Lower damping factor ratio

The first and second dampers are set to 0.4 Ns/m and 0.05 Ns/m respectively. When the damping factor ratio c_2/c_1 is equal to 0.125, the response magnitudes of mass are shown in time domain in Figure 4.15;

- Response time will increase
- Displacement of primary mass will increase (c_1 $constant$)
- Displacement of secondary mass will increase (c_2 $decrease$)

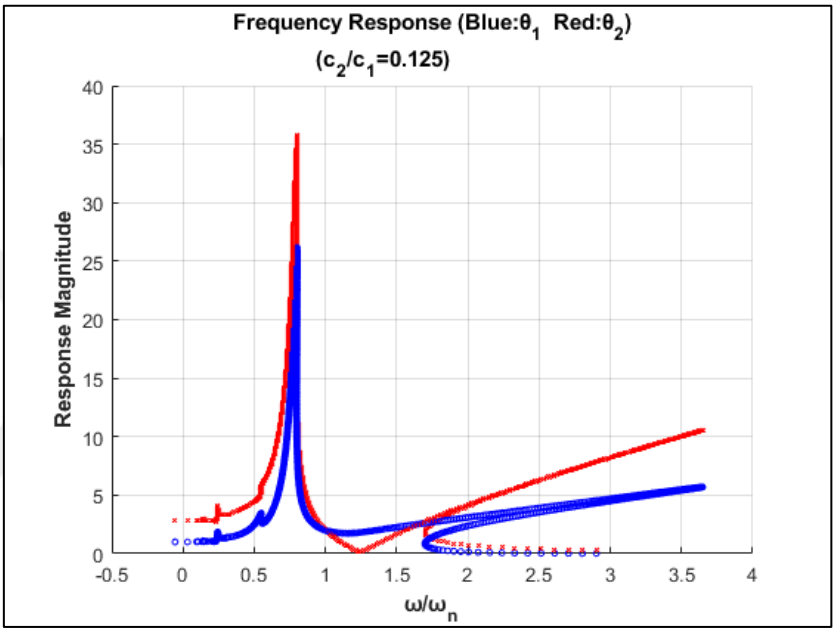

Figure 4.15: Displacement in time domain (c_2/c_1=0.125) (a)full-scale (b)zoomed.

To understand clearly, system damping modifications and their effects are shown in below Table 4.7;

Table 4.7: The damping ratio effect on $\boldsymbol{\theta_1}$ and $\boldsymbol{\theta_2}$ displacements.

Test Number	c_2/c_1	θ_1	θ_2	Peak Frequency
0	0.25	25.453	34.868	0.799
1	0.5	24.132	33.162	0.796
2	0.125	26.155	35.805	0.801

The second important parameter of the system is damping ratio. In this comparison, main flywheel body is kept constant, and all changes are applied on secondary mass. Dual mass can be chosen a material which has less or more damping performance.

In first case, damping ratio is high, main flywheel and secondary body displacement will decrease 5%, and the frequency which is seen peak amplitude is kept same for all damping ratio case.

When the damping coefficient of the secondary mass on the transmission side has a lower value, the displacements increase 5% according to initial condition. Like test-1, peak frequency is same in test-2.

If the primary mass is manipulated in terms of damping coefficient, the change of stabilize response time will dramatically increase or decrease. Hence, it is clearly understood that the damping of primary mass is more dominant on system.

The damping of secondary mass has also important role on response magnitude around 2nd natural frequency. While damping ratio increase, the response magnitude of both mass decrease around 2nd natural frequency. In contrast, when secondary mass has less damp characteristic, the magnitudes increase around 2nd natural frequency. Damping ratio has no significant effect on 2nd natural frequency value.

4.2.3 The stiffness ratio effect (k_1/k_2)

4.2.3.1 Higher stiffness ratio

The first and second stiffness ratios are set to 600 Ns/m and 150 Ns/m respectively. When the damping factor ratio k_1/k_2 is equal to 4, the response magnitudes of mass are shown in time domain in Figure 4.16;

- The amplitude of primary mass will slightly increase ($k_1\ constant$)
- The amplitude of secondary mass will slightly increase ($k_2\ decrease$)

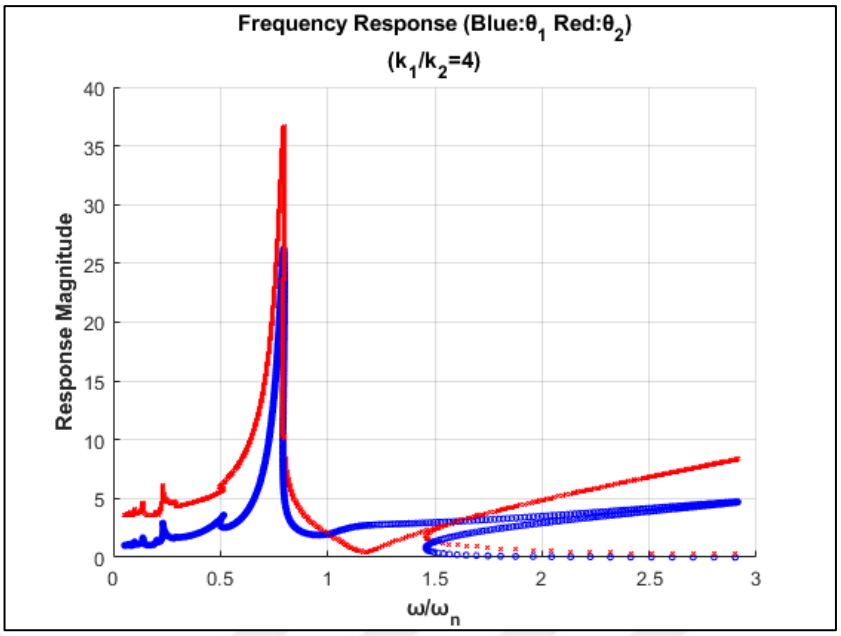

Figure 4.16: Displacement in frequency domain (k_1/k_2=4).

4.2.3.2 Lower stiffness ratio

The first and second stiffness ratios are set to 600 Ns/m and 450 Ns/m respectively. When the damping factor ratio k_1/k_2 is equal to 1.3, the response magnitudes of mass are shown in time domain in Figure 4.17;

- The amplitude of primary mass will increase (k_1 $constant$)
- The amplitude of secondary mass will increase (k_2 $increases$)

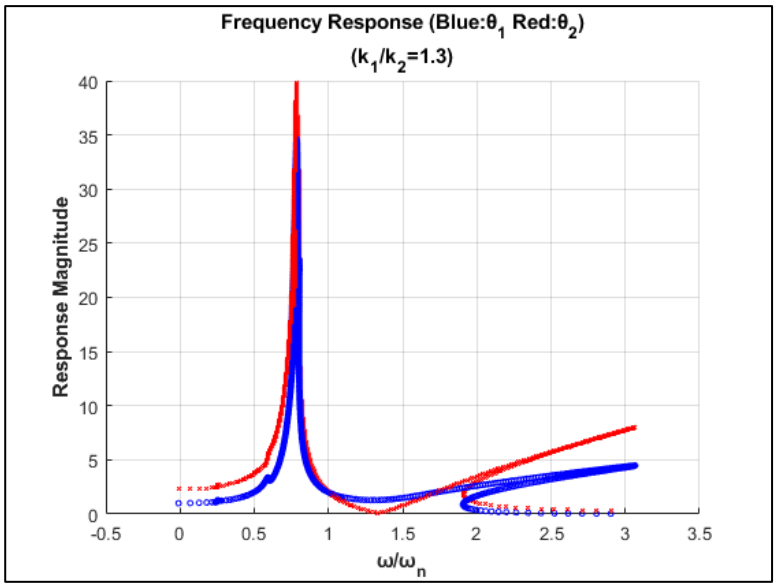

Figure 4.17: Displacement in frequency domain (k_1/k_2=1.3).

To understand clearly, system stiffness modifications and their effects are shown in below Table 4.8;

Table 4.8: The stiffness ratio effect on $\boldsymbol{\theta_1}$ and $\boldsymbol{\theta_2}$ displacements.

Test Number	k_1/k_2	θ_1	θ_2	Peak Frequency
0	2	25.453	34.868	0.799
1	4	26.265	33.629	0.796
2	1.3	34.596	39.797	0.786

The third important parameter of the system is stiffness ratio. In this comparison, transmission side is kept constant, and all changes are applied on ICE side. Thus, primary stiffness coefficient can be chosen as a have less or more stiff material.

In first case, stiffness ratio is high, main and secondary mass displacement will increase 3-5%. Furthermore, the peak amplitude frequencies of two mass are same according to initial case.

Secondary mass can be used in more stiff material as second case. In this case, stiffness ratio (k_1/k_2) is low, primary and secondary body displacements will slightly increase as 3%. Besides, the peak amplitude frequencies of two mass are same as other case.

Moreover, as the secondary mass has stiffer characteristic, the response magnitude slightly increases around 2nd natural frequency. If secondary mass has less stiff characteristic, the magnitude slightly decreases. Also, 2nd natural frequency value increases as stiffness of second mass increases.

4.2.4 The non-linear stiffness ratio effect (α)

The non-linear stiffness ratio is set to 0.01, 0.5, and at last 0 which means linear system.

4.2.4.1 Higher non-linear stiffness ratio

The non-linear stiffness ratio is set to 0.5, the response magnitudes of mass are shown in time domain in Figure 4.18;

- Peak frequency will slightly increase
- Displacement of primary mass will increase
- Displacement of secondary mass will decrease

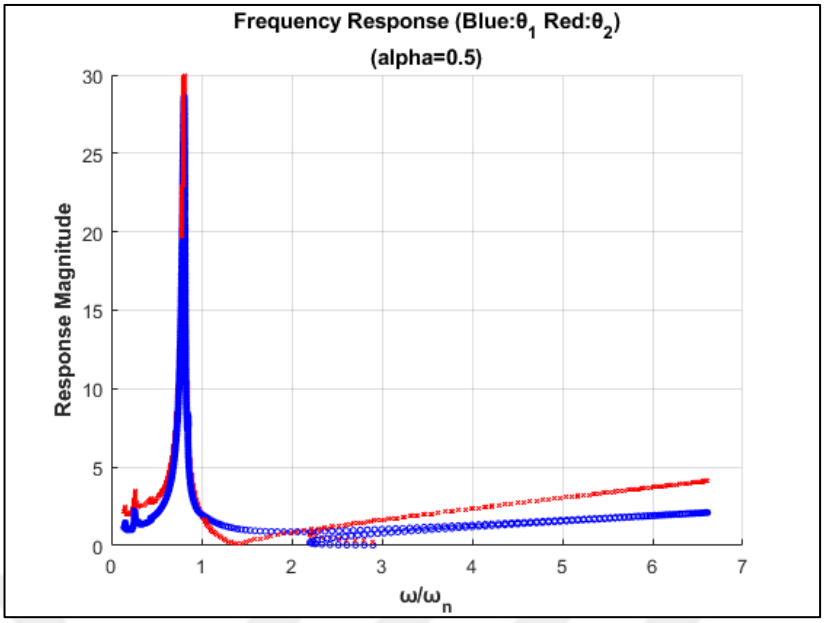

Figure 4.18: Displacement in frequency domain (alpha=0.5).

4.2.4.2 Lower non-linear stiffness ratio

The non-linear stiffness ratio is set to 0.01, the response magnitudes of mass are shown in time domain in Figure 4.19;

- Peak frequency will slightly decrease
- Displacement of primary mass will increase
- Displacement of secondary mass will increase

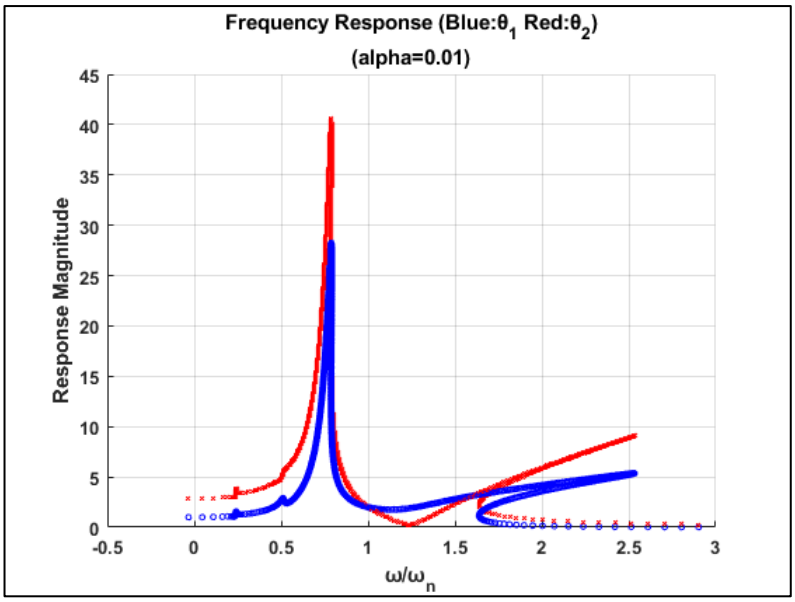

Figure 4.19: Displacement in frequency domain (alpha=0.01).

4.2.4.3 Zero non-linear stiffness ratio

The non-linear stiffness ratio is set to 0, the response magnitudes of mass are shown in time domain in Figure 4.20;

- Peak frequency will decrease
- Displacement of primary mass will increase
- Displacement of secondary mass will dramatical increase

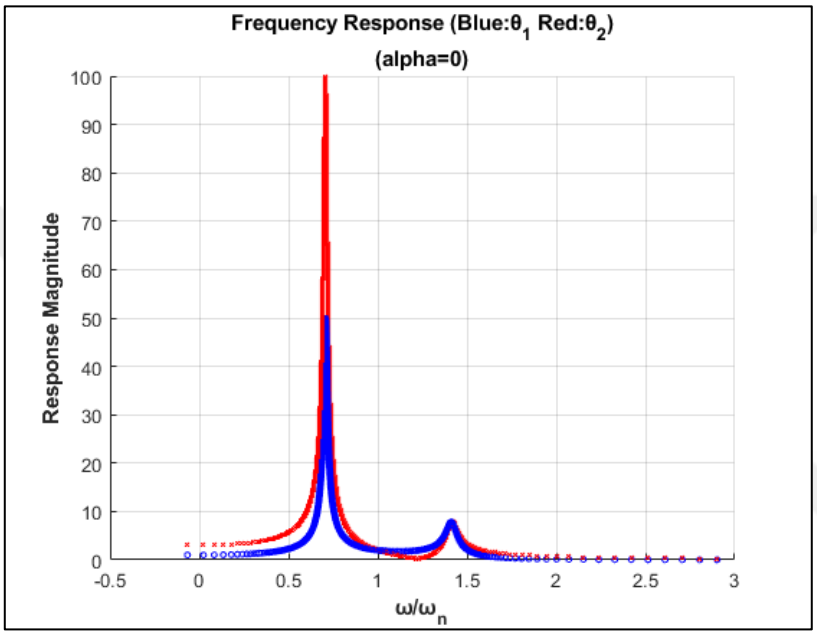

Figure 4.20: Displacement in Frequency Domain (alpha=0).

To understand clearly, non-linear stiffness ratio modifications and their effects are shown in below Table 4.9;

Table 4.9: The non-linear stiffness ratio effect on $\boldsymbol{\theta_1}$ and $\boldsymbol{\theta_2}$ displacements.

Test Number	α	θ_1	θ_2	Peak Frequency
0	0.02	25.453	34.868	0.799
1	0.5	28.642	29.913	0.807
2	0.01	28.256	40.667	0.789
3	0	49.949	99.978	0.707

Another important parameter of the system is non-linear stiffness ratio. For the first case, non-linear ratio is considered as 0.5 which means higher non-linear stiffness coefficient than initial case. In this case, displacement of main body increases as 13%,

while secondary body has less angular displacement as 14%. The peak amplitudes of two masses are at higher frequency value according to initial case.

For the second case, non-linear stiffness ratio is considered as 0.01 which means lower non-linear stiffness coefficient than initial case. For this case, displacement of main body and secondary body increase, because of getting system less stiff. Unlike test-1, the peak frequency is shifted to lower value in test-2.

For the last case off non-linearity test is that equal to zero which means system has linear characteristic. In test-3, non-linear stiffness ratio will be adjusted to zero. The primary mass displacement is dramatically increase like %100. The secondary mass has also increase as 186%.

The non-linear stiffness coefficient is another important parameter for response magnitude around 2^{nd} natural frequency. While alpha increase from 0.02 to 0.5, the response magnitude of both mass increase around 2^{nd} natural frequency. In contrast, when alpha decrease from 0.02 to 0.01, the magnitudes decrease around 2^{nd} natural frequency. In addition, 2^{nd} natural frequency value increases as alpha also increases. For linear situation which means alpha equal to zero, 2^{nd} natural frequency decreases approximately from 1.7 to 1.4 and also magnitudes also decrease.

5. CONCLUSIONS AND RECOMMENDATIONS

The one of the solutions for torsional vibration are the using of dual mass flywheel. In this paper, a simplified DMF model has been examined in Matlab with manipulated different parameter. The aim of all modifications is that having better damping performance from engine to transmission system.

All changes are applied on DMF mathematical model was investigated in time domain. For all graphs, while blue curves presented secondary mass and transmission output, orange curves presented primary mass and effect of ICE.

After modifying all the parameters in the system, it showed that the angular displacements of the primary and secondary mass decreases as the stiffness coefficient decreases. On the other hand, when the stiffness coefficient of secondary mass increases, ICE should be had more fluctuations for same output to transmission. Moreover, the system damping ratio increases, the bodies has less angular movement. If displacements would like to be decreased, inertia ratio (secondary mass inertia) should be decreased.

When the non-linear stiffness effect increases on system, angular displacements of bodies decrease. In contrast, less non-linear stiffness coefficient leads to more body displacements according to initial case.

Increasing damping coefficient of secondary mass affect positively on system. The high damping coefficient reduces time to stable output amplitude. However, the lower inertia ratio means that less time to need stabilization.

Likewise, all parameter changes made on the system are also examined in the frequency domain. For all graphs in frequency domain, blue curves presented primary mass and red curves presented secondary mass.

All modifications in 2DOF system are done to examine effect of parameters on DMF. All the results mentioned in this paragraph are interpretations of the outputs obtained at the first natural frequency of the system. When inertia ratio is high value, the response amplitude is also high for both masses. However, if the inertia value of the

second mass is decreased, the second mass decreases even if the response magnitude of the first mass increases. The damping ratio of the system is manipulated by adjusting with the damping coefficient of the secondary mass. The results show that as the damping ratio increases, that is, the damping coefficient of the secondary mass increases, the response amplitude of the system decreases. On the contrary, as the damping ratio of the system decreases, that is, the damping coefficient of the second mass decreases, the response amplitude of the system increases. The stiffness ratio of the system is manipulated by changing the stiffness coefficient of the secondary mass. Obtained results show that as the stiffness ratio increases, that is, as the stiffness coefficient of the secondary mass is decreased, the response amplitude of the secondary mass slightly decreases. On the contrary, as the stiffness of the system decreases, that is, as the stiffness coefficient of the secondary mass increases, the response amplitude of the system increases.

At 2^{nd} natural frequency region, the response amplitude of the system and the value of the 2nd natural frequency decreased as the inertia ratio increased. On the contrary, the lower the inertia ratio, the higher the 2nd natural frequency value. However, while the response amplitude of the 2nd mass increases, the response amplitude of the 1st mass decreases. Moreover, the system response amplitudes decrease as the damping ratio increases, although the second natural frequency remains constant. Conversely, the amplitudes increase as the damping ratio decreases. As the stiffness of the system increases, the second natural frequency value and the system response amplitude decrease. In contrast, as the stiffness ratio decreases, the natural frequency value and the system response amplitude increase. The last parameter is the nonlinear stiffness coefficient. As this coefficient decreases, the amplitude and natural frequency value decrease. If the non-linear stiffness coefficient increases, the system response magnitude and natural frequency value increase. In the linear position of the system, that is, when the nonlinear coefficient is equal to zero, the amplitudes and the second natural frequency value decrease. Since the system is linear, there is a system response for each frequency.

REFERENCES

[1] **Şen, O.T., Singh, R.** (2018). Energy exchange between two sub-systems coupled with a nonlinear elastic path, *Noise and vibration emerging methods: 6th conference. Ibiza, Spain*

[2] **Güllü, E., Yılmaz, A.** (2020). Influence of single and dual mass flywheel usage in ic engines on clutch dynamics, *International Journal of Automotive Science and Technology* **(**Vol. 4, pp.40-48). doi:10.30939/ijastech..678615.

[3] **Chen, L., Shi, W., Chen, Z.,** (2020). Reseasrch on damping performance of dual mass flywheel based on vehicle transmission system modelling and multi-condition simulation, *National Key R&D Program of China, China.*

[4] **Reik, W., Seebacher, R., Kooy, A.,** (n.d). Dual mass flywheel, Retrieved from https://www.schaeffler.com/remotemedien/media/_shared_media/08_media_library/01_publications/schaeffler_2/symposia_1/downloads_11/4_DMFW_1.pdf *National Key R&D Program of China, China.*

[5] **Bourgois, G.** (2016). *Dual mass flywheel for torsional vibrations damping*. Chalmers University of Technology, Department of Applied Mechanics, GOTHENBURG.

[6] **Saygılı, Y.** (2018). *Torsional vibrations of gear systems with single and dual mass flywheels: modelling and analyses*. Istanbul Technical University, Department of Mechanical Engineering, ISTANBUL.

[7] **Yılmaz, A.** (2019). *İçten yanmalı motorlarda çift kütleli volan kullanımı ve taşıt güç aktarma sisteminin performansına etkileri.* Bursa Uludağ Üniversitesi, Makine Mühendisliği Anabilim Dalı, BURSA.

[8] **Galvagno, E., Vigliani, A. and Calenda, G.,** (2020). "Dual-Mass Flywheel with Torque Limiter: An Effective Solution for Overtorque Suppression in Automotive Transmission," SAE Technical Paper, doi:10.4271/2020-01-1016.

[9] **Johansson, D., Karlsson, K.,** (2017). *Simulation models of dual mass flywheels*. Chalmers University of Technology, Department of Applied Mechanics, GOTHENBURG.

[10] **Bucha, J., Danko, J., Milesich, T., Mitrovic, R., Miskovic, Z.,** (2020). Dynamic simulation of dual mass flywheel. China Chongqing University, College of Mechanical Engineering, CHINA.

[11] **Zeng, L., Huang, J., Xu, Y., Song, L.,** (2021). Modeling and dynamics analysis of a dual-mass flywheel with the conformal contact action of friction damping ring and pressure plate. *Spring Nature Switzerland, 90, 375*-392. doi:10.1007/978-3-030-30853-7_22.

[12] ***Geislinger Coupling.*** *(2018).* Coupling catalog version 17.9. *Retrieved November 21, 2022, from* https://www.geislinger.com/

[13] **Song, L.Q., Zeng, L.P., Zhang, S.P., Zhou, J.D., Niu, H.E.,** (2014). Design and analysis of a dual mass flywheel with continuously variable stiffness based on compensation principle. China Chongqing University, College of Electronic Engineering, CHINA

Url-1 < https://valeoservice.cld.bz/VS-Transmission-Systems-Dual-Mass-Flywheel-DMF-valeoscope> , data retrieved 21.11.2022

CURRICULUM VITAE

Name Surname : Gökay Karakuş

EDUCATION :

- **B.Sc. :** 2016, Istanbul Technical University, Mechanical Engineering Department, Mechanical Engineer
- **M.Sc. :** 2023, Istanbul Techincal University, Mechanical Engineering Faculty, Automotive

PROFESSIONAL EXPERIENCE AND REWARDS:

- 2023- Ford Otomotiv Sanayi A.Ş., HCV Structural Systems Design Engineer
- 2019-2022 Bmcpower Motor Kontrol ve Teknolojileri A.Ş., Engine Development, Cylinder Block System, Design Engineer